1976

DEPOLARIZATION OF DOUBLET-6P CESIUM ATOMS INDUCED IN COLLISIONS WITH NOBLE GASES.

JOHN. GUIRY

University of Windsor

INFORMATION TO USERS

THIS DISSERTATION HAS BEEN
MICROFILMED EXACTLY AS RECEIVED

This copy was produced from a micro-
fiche copy of the original document.
The quality of the copy is heavily
dependent upon the quality of the
original thesis submitted for
microfilming. Every effort has
been made to ensure the highest
quality of reproduction possible.

PLEASE NOTE: Some pages may have
indistinct print. Filmed as
received.

AVIS AUX USAGERS

LA THESE A ETE MICROFILMEE
TELLE QUE NOUS L'AVONS RECUE

Cette copie a été faite à partir
d'une microfiche du document
original. La qualité de la copie
dépend grandement de la qualité
de la thèse soumise pour le
microfilmage. Nous avons tout
fait pour assurer une qualité
supérieure de reproduction.

NOTA BENE: La qualité d'impression
de certaines pages peut laisser à
désirer. Microfilmée telle que
nous l'avons reçue.

DEPOLARIZATION OF 6^2P CESIUM ATOMS

INDUCED IN COLLISIONS WITH

NOBLE GASES

by

JOHN GUIRY

A Dissertation
Submitted to the Faculty of Graduate Studies through the
Department of Physics in Partial Fulfillment of the
Requirements for the Degree of Doctor of Philosophy
at the University of Windsor

Windsor, Ontario
1975

ABSTRACT

Modified Zeeman scanning techniques were used to determine cross sections for depolarization of $6^2P_{1/2}$ and $6^2P_{3/2}$ Cs atoms, induced in collisions with noble gas atoms in their ground states.

Cross sections σ_1, for disorientation of $^2P_{1/2}$ Cs atoms induced in collisions with He, Ne, Ar, Kr and Xe were determined at a magnetic field of 9.8 kG and were found to be considerably larger than values reported at zero field (Bulos and Happer 1971). Consequently a systematic study was carried out of the effect of magnetic field on σ_1 for Cs $(^2P_{1/2})$ He collisions, in the range 0 - 10 kG. σ_1 was found to increase with magnetic field, and the effect can not be explained on the basis of nuclear decoupling since in kilogauss magnetic fields $\vec{I}$ and $\vec{J}$ are already effectively decoupled. On the other hand, the cross sections obtained at zero field were extracted from experimental data using a treatment which takes coupling effects into account. The effects of the magnetic field on the σ_1 cross sections is ascribed to field-induced virtual fine-structure $^2P_{1/2}$ - $^2P_{3/2}$ mixing (Baylis 1971) and is found to be in reasonable agreement with theoretical predictions (Baylis 1975).

Depolarization of the $6^2P_{3/2}$ state of Cs induced in collisions with He, Ne, Ar, and Xe buffer gas atoms was also investigated. The cross sections for the destruction

of circular and linear polarization, Q(circ.) and Q(lin.) respectively, as well as cross sections for disorientation (σ_1) and disalignment (σ_2) were obtained. In the absence of hfs, Q(circ.) and Q(lin.) are representative of σ_1 and σ_2, respectively. By decoupling of the atomic and nuclear spins in a kilogauss magnetic field the role played by the nuclear spin in the relaxation process was studied and was found to be considerably more pronounced in the case of circular depolarization than linear depolarization. The results obtained are in reasonable agreement with other theoretical and experimental results.

ACKNOWLEDGEMENTS

TABLE OF CONTENTS

vii

LIST OF TABLES

LIST OF FIGURES

x

I. INTRODUCTION

With the advent of optical pumping more than two decades ago, the collisionally induced relaxation of atomic ground states has become the subject of widespread investigation. More recently, such relaxation studies have been extended to include various excited states. Considerable attention has been focused on the depolarization of excited alkali atoms induced in collisions with ground-state noble gas atoms. Such systems are relatively uncomplicated and are amenable to experimental and theoretical treatment.

An atomic ensemble is said to be polarized if a non-random population distribution exists among the various Zeeman substates. The population distribution is given by the diagonal elements of the density matrix (non-diagonal matrix elements represent coherences between the various Zeeman substates, which will not be considered in this dissertation) and consequently the dimension of the density matrix is $2J+1$, the number of Zeeman substates of a state with total electronic angular momentum quantum number J in the absence of hyperfine structure (hfs).

The density matrix formalism (Fano 1957; Omont 1965; D'Yakanov and Perel' 1965 a,b,c) facilitates the calculation of average values of the atomic observables. The density matrix can be expanded in terms of irreducible tensor operators, each corresponding to one of the

1

multipole moments of the population distribution. The polarization of the atomic ensemble can thus be specified on the basis of the multipolarity of such population distributions. The terms "orientation" and "alignment" refer, for instance, to the dipole and quadrupole population moments, respectively. An orientation, characterized by the presence of a net magnetic moment along the axis of quantization, is said to exist when those substates with magnetic quantum numbers of the same sign are preferentially populated. Alignment is present when substates having magnetic quantum numbers of the same absolute value are populated preferentially. Collisions with noble gas atoms will relax each such multipole moment with a relaxation rate which may differ from one multipole to another. Thus, for the $^2P_{\frac{1}{2}}$ and $^2P_{3/2}$ alkali resonance states, there are two and four relaxation rates, respectively. They are γ_0 (relaxation of the excited state population), γ_1 (relaxation of the dipole moment or of orientation), γ_2 (relaxation of the quadrupole moment or of alignment) and γ_3 (relaxation of the octupole moment), and all can be, in principle, determined experimentally. The $^2P_{\frac{1}{2}}$ state can possess only orientation and only γ_0 and γ_1 can be determined for it. The $^2P_{3/2}$ state, on the other hand, may have both orientation and alignment, and its relaxation is subject to all four relaxation rates.

The values of γ_1 depend on the type of interaction involved in the depolarization process. If relaxation is

caused by 'hard collisions' when the distance of approach is close and the collision time short, the various multipole relaxation rates are equal. In this case the 'J randomization' mechanism is thought to apply in which the orientation of $\vec{J}$ is completely randomized by the collision. If, on the other hand, the collisions are 'soft' (long range and long collision time), then $\gamma_1 = \frac{\gamma_2}{2} = \gamma_3$ (Happer 1972). If the Van der Waals' model of dynamic polarization is used with straight collision trajectories to treat the collisions, then $\gamma_1 : \gamma_2 : \gamma_3 \doteq 0.92 : 1.14 : 1.01$ (Okunevich and Perel' 1970).

When considering collision-induced depolarization of excited alkali atoms, it should be borne in mind that they all possess nuclear spin and, consequently, it is necessary to consider the processes of excitation, spontaneous decay and collisional relaxation in the presence of hyperfine structure. Considerable simplification is afforded in this respect by the 'nuclear decoupling approximation', originally introduced by Bender (1956) and subsequently verified by Papp and Franz (1972), according to which the nuclear angular momentum is considered to remain undisturbed during the collision while the electronic angular momentum may suffer reorientation. The duration of the collision should therefore be much shorter than the hyperfine period, if the nuclear spin $\vec{I}$ is to remain unaffected, and should be comparable to or greater than the fine structure period if the electronic angular momentum $\vec{J}$ is to be reoriented:

(I-1) $\qquad \tau_c \ll \tau_{hf}$

(I-2) $\qquad \tau_c \geq \tau_f$

where τ_c is the duration of the collision, τ_{hf} is the hyper-fine period and τ_f, the fine structure period. Because after the collision $\vec{I}$ and $\vec{J}$ recouple, the time between collisions τ_{coll} must not be shorter than the hyperfine period:

(I-3) $\qquad \tau_{coll} \geq \tau_{hf}$

Each of these characteristic times must, of course, be smaller than τ, the lifetime of the excited state, except for τ_{coll}:

(I-4) $\qquad \tau_f < \tau_c < \tau_{hf} < \tau < \tau_{coll}.$

It may be seen in Table 1, which contains representative values of these various quantities for the first excited states of the alkali atoms, that Condition (I-4) is satis-fied only for the first excited states of Rb and Cs.

The collision itself is simplified by the use of the nuclear decoupling approximation but the subsequent re-coupling of the electronic and nuclear moments after the collision significantly affects the relaxation rates, which are all diminished in comparison to those that would be observed for atoms with I=0. In addition, the various multipole moments no longer relax independently, so that a unique relaxation rate, corresponding to a particular multi-pole moment, can not be determined. If specific relaxation rates are required, the complexity introduced by the influ-ence of the nuclear spin must in some way be eliminated.

TABLE 1   Characteristic periods for collisions between Alkali Atoms in their first excited states and ground state noble gas atoms (time expressed in sec.)

Alkali	τ_f	τ_c	τ_{hf}	τ	$\tau_{coll.}$
Na	10^{-12}	10^{-12}	10^{-8}	10^{-8}	$10^{-7}-10^{-8}$
K	10^{-12}	10^{-12}	10^{-8}	10^{-8}	"
Rb	10^{-13}	10^{-12}	10^{-9}	10^{-8}	"
Cs	10^{-13}	10^{-12}	10^{-9}	10^{-8}	"

Depolarization of atomic fluorescence, induced by collisions with ground-state noble gas atoms has been subjected to extensive experimental investigations, beginning with R.W. Wood (1922, 1923) and W. Hanle (1927) who studied the collisional depolarization of mercury and sodium atoms even before nuclear spin had been shown to exist. More recent studies of excited state depolarization in alkali atoms are listed in Table 2.

General theoretical treatments of collisional relaxation of excited atoms have been proposed by D'Yakonov and Perel' (1965), Omont (1965) and Wang and Tomlinson (1969). In the particular case of excited alkali atoms, Franz and Franz (1966) suggested two models for the depolarization process, one involving a random reorientation of the total electronic angular momentum and the other governed by a selection rule for Zeeman transitions: $\Delta m_J = 0, \pm 2$. Elbel and Naumann (1967 a,b,) obtained the selection rule $m_J \neq -m_J$ for

TABLE 2

Experimental Studies of ^2P Collisional
Depolarization in Alkali Atoms

Atomic State	Experimental Method	Reference
Rb $5^2P_{\frac{1}{2}}$	Optical Pumping	Marrus and Yellin 1966
Cs $6^2P_{3/2}$	Optical Pumping	Fricke et al. 1967
Rb $5^2P_{3/2}$	Optical Pumping	Zhitnikov et al. 1969
Rb $5^2P_{3/2}$	Optical Pumping	Papp and Franz 1972
Cs $6^2P_{\frac{1}{2}}$	Optical Pumping	Franz & Sooriamoorthi 1974
Rb $5^2P_{\frac{1}{2}}, {}^2P_{3/2}$	Hanle Effect	Gallagher 1967
Cs $6^2P_{\frac{1}{2}}$	Hanle Effect	Gallagher 1967
Cs $6,7^2P_{3/2}$	Hanle Effect	Markova and Chaika 1967
Cs $7^2P_{\frac{1}{2}}, {}^2P_{3/2}$	Hanle Effect	Altman and Evdokimov 1970
Rb $5^2P_{\frac{1}{2}}$	Hanle Effect	Bulos and Happer 1971
K $4^2P_{\frac{1}{2}}$	Zeeman Scanning	Berdowski and Krause 1968
K $4^2P_{3/2}$	Zeeman Scanning	Berdowski et al. 1971
Na $3^2P_{\frac{1}{2}}$	Depolarization of fluorescence	Niewitecka et al. 1974
K $4^2P_{\frac{1}{2}}$	Depolarization of fluorescence	Niewitecka and Krause 1975
Rb $5^2P_{3/2}$	Depolarization of fluorescence	Kamke 1975

mixing within a J multiplet state by treating the mixing of the Zeeman substates as being due to collisional phase shifts between the molecular Σ and Π substates into which the atomic ^2P state is split during the collision. Subsequent calculations by Mandelberg (1968) did not indicate the existence of such selection rules. Gordeev et al. (1969) treated the depolarization of the $^2P_{\frac{1}{2}}$ state by postulating a quasi-molecular complex, in which the depolarization was caused by Coriolis mixing of adiabatic electronic molecular states, whereas depolarization in the $^2P_{3/2}$ state was due to dipole-dipole interactions. This model was subsequently extended by Roueff and Suzor (1974), who considered the nuclear and electronic spins to be effectively decoupled. Okunevich and Perel' (1970) treated depolarization in the $^2P_{3/2}$ states of Rb and Cs in the context of the density matrix formalism, assuming a van der Waals' model for the interaction.

The specific effect of nuclear spin inertia on the results of Hanle effect experiments was considered by Bulos and Happer (1971). Gallagher had used this method to study the disorientation of $5^2P_{\frac{1}{2}}$ Rb and $6^2P_{\frac{1}{2}}$ Cs atoms, induced by collisions with noble gases. The resulting cross sections were very small compared with the cross sections for depolarization in the corresponding $^2P_{3/2}$ states as was to be expected, considering the magnitude of the fine structure splitting in Rb and Cs. However, the effect of the nuclear

spin inertia is to narrow the Hanle curves and change the dependence of their widths on noble gas pressure from a linear to a quasi-linear one. This effect is independent of any electronic depolarization process and causes the disorientation cross section to be severely underestimated. Bulos and Happer (1971) reanalyzed Gallagher's (1967) measurements, making due allowance for the nuclear spin inertia, and obtained values for the disorientation cross sections that were larger than Gallagher's original values by a factor of at least 3. Although they did not carry out specific calculations for the $^2P_{3/2}$ state, it should be expected that the depolarization cross sections will be similarily affected (Happer 1972).

The analysis of data determined in optical pumping experiments has yielded important information on the collisional relaxation processes. The resulting relaxation rates depend, however, on the particular model assumed for the excited state mixing (e.g. J randomization, J randomization subject to m_J selection rules etc.) and they also include nuclear spin effects for which, however, appropriate corrections can be made. Thus Fricke et al. used 'D$_2$ optical pumping' to measure depolarization cross sections for the $6^2P_{3/2}$ state of Cs, assuming the "J randomization model". Papp and Franz also used D$_2$ optical pumping to measure collisional relaxation rates in the $5^2P_{3/2}$ state of Rb, and obtained virtually the same results for both isotopes, in accord with the 'nuclear decoupling approximation', for

which their work provided experimental verification. The depolarization cross sections which they determined by assuming a van der Waals interaction were considerably larger than those previously obtained by Gallagher. Similar results were also obtained by Zhitnikov et al. (1970). The cross sections determined by these two groups were found to be larger than Gallagher's values, irrespectively of the interaction model that was assumed.

Franz and Sooriamoorthi (1974) derived expressions for the quasi-equilibrium orientation of $^2P_{1/2}$ alkali atoms, corrected for nuclear spin, and used them in an analysis of D_1 optical pumping rates. Their treatment may also be employed to determine the nuclear spin - independent disorientation cross section from experiments on depolarization of resonance fluorescence at zero field.

A different problem is encountered when considering the collision induced orientation and disalignment of $^2P_{3/2}$ alkali atoms. Rebane and Rebane (1973) have considered the collisional depolarization of such atoms possessing hyperfine structure, using perturbation theory based on a series expansion of the density matrix in powers of buffer gas pressure and assuming the van der Waals' model for the interaction. They determined the role of the various multipole moments in the relaxation process and related the observed relaxation rates to those that would be obtained in the absence of hyperfine structure.

In the present investigation, modified Zeeman scanning techniques were used to determine cross sections for depolarization of $6^2P_{1/2}$ and $6^2P_{3/2}$ Cs atoms, induced in col-

lisions with noble gas atoms in their ground states. The
experiments were carried out in magnetic fields ranging from
zero to 10 kG. At low fields where $\vec{I}$ and $\vec{J}$ remain coupled,
the results for the $^2P_{1/2}$ state were corrected for nuclear
spin, to yield disorientation cross sections. At higher
fields, it is possible to probe the effect of the magnetic
field on the cross sections. In the case of the $^2P_{3/2}$ state,
cross sections for both circular and linear depolarization
were obtained which, at high fields, are representative of
the disorientation and disalignment cross sections, respectively.

The advantage of the Zeeman scanning method in
which the depolarization of resonance fluorescence is moni-
tored in relation to buffer gas pressure, lies in the fact
that it leads directly to specific depolarization cross
sections which can be extracted from the experimental data
without any assumptions concerning interaction mechanisms.
In magnetic fields sufficiently strong to decouple $\vec{I}$ and $\vec{J}$,
no corrections for the nuclear spin effect need be applied
to the data and the resulting disorientation and disalignment
cross sections can be directly compared with theoretical
calculations, permitting less ambiguous conclusions than can
be obtained from results produced by most other methods.

II.   THE PRINCIPLE OF ZEEMAN SCANNING

Zeeman scanning is a technique in which the wave-length of light incident on an absorbing medium is varied continuously by placing the light source in a variable magnetic field. If all but one of the resulting Zeeman components are removed by the interposition of a suitable filter, the remaining component may then be used to probe the absorption profile in the gas or vapour under investigation (Bitter et al. 1954). The procedure may also be reversed, with the variable magnetic field applied to the absorbing sample instead of the light source (Buhl 1938).

In the present investigation I have used a modified Zeeman scanning technique, with two separate and independently adjustable magnetic fields M_1 and M_2. The spectral lamp was located in the field M_1 and the fluorescence cell in M_2. In this way the resonance lines emitted by the lamp and the absorption lines in the fluorescing vapour are split independently into their Zeeman components. With the aid of suitable polarizers, various Zeeman components can be selectively excited in fluorescence and the rate of collisional population transfer among the Zeeman sublevels can be investigated by monitoring the change in the polarization of the resonance fluorescence.

1. Selective Excitation of the $m_J = -1/2$, $m_I = -7/2$ Zeeman Sublevel of the Cs $6^2P_{1/2}$ State

The optical excitation of the $m_J = -1/2$ Zeeman sublevel in the Cs($6^2P_{1/2}$) atoms proceeds as follows. 8943-Å

11

radiation emitted by a cesium spectral lamp is made incident on low-pressure cesium vapour contained in a fluorescence cell and placed in a magnetic field which can be varied from 0 to 10 kG. Excitation takes place with the unpolarized incident beam of light directed perpendicularly to the field while the flourescent light is observed parallel to the field. Figure 1 shows the Zeeman splitting of the 8943-$\overset{o}{A}$ absorption line in relation to the magnetic field. The pattern consists of two sets of π and σ components, each set being split further into several hyperfine structure components due to the nuclear spin. In cesium, which is monoisotopic and has a nuclear-spin quantum number 7/2, the hfs of each π or σ set consists of eight components. The π components arising from $m_J=-\frac{1}{2} \rightarrow m_J=-\frac{1}{2}$ transitions are designated as π^- and those arising from $m_J=+\frac{1}{2} \rightarrow m_J=+\frac{1}{2}$ transitions are designated as π^+ ; the designation σ^+ and σ^- refer to $m_J=-\frac{1}{2} \rightarrow m_J=+\frac{1}{2}$ and $m_J=+\frac{1}{2} \rightarrow m_J=-\frac{1}{2}$ transitions, respectively. The hyperfine lines are specified by designating the value of m_I for the levels involved, e.g., the transitions $m_I=-7/2 \rightarrow m_I=-7/2$ are labelled -7/2.

As the field surrounding the cell is increased, various coincidences occur between the frequencies of the hyperfine components emitted from the lamp and the absorption frequencies of the π lines, resulting in the excitation of hyperfine sublevels of both the $m_J=+\frac{1}{2}$ and $m_J=-\frac{1}{2}$ substates. As may be seen in Figure 2 at a field of 9.8 kG, the 0.1889

Figure 1.   The magnetic splitting of the 8943-Å absorption
line in the range 0 - 10 kG, as calculated from the Breit-Rabi
Equation (Breit and Rabi 1931).   The solid and dashed lines indi-
cate σ and π components, respectively. σ components arise from
$\Delta m=\pm 1$ transitions; π components, from $\Delta m=0$ transitions.   m is
the projection of the total atomic angular momentum on the axis
of quantization.
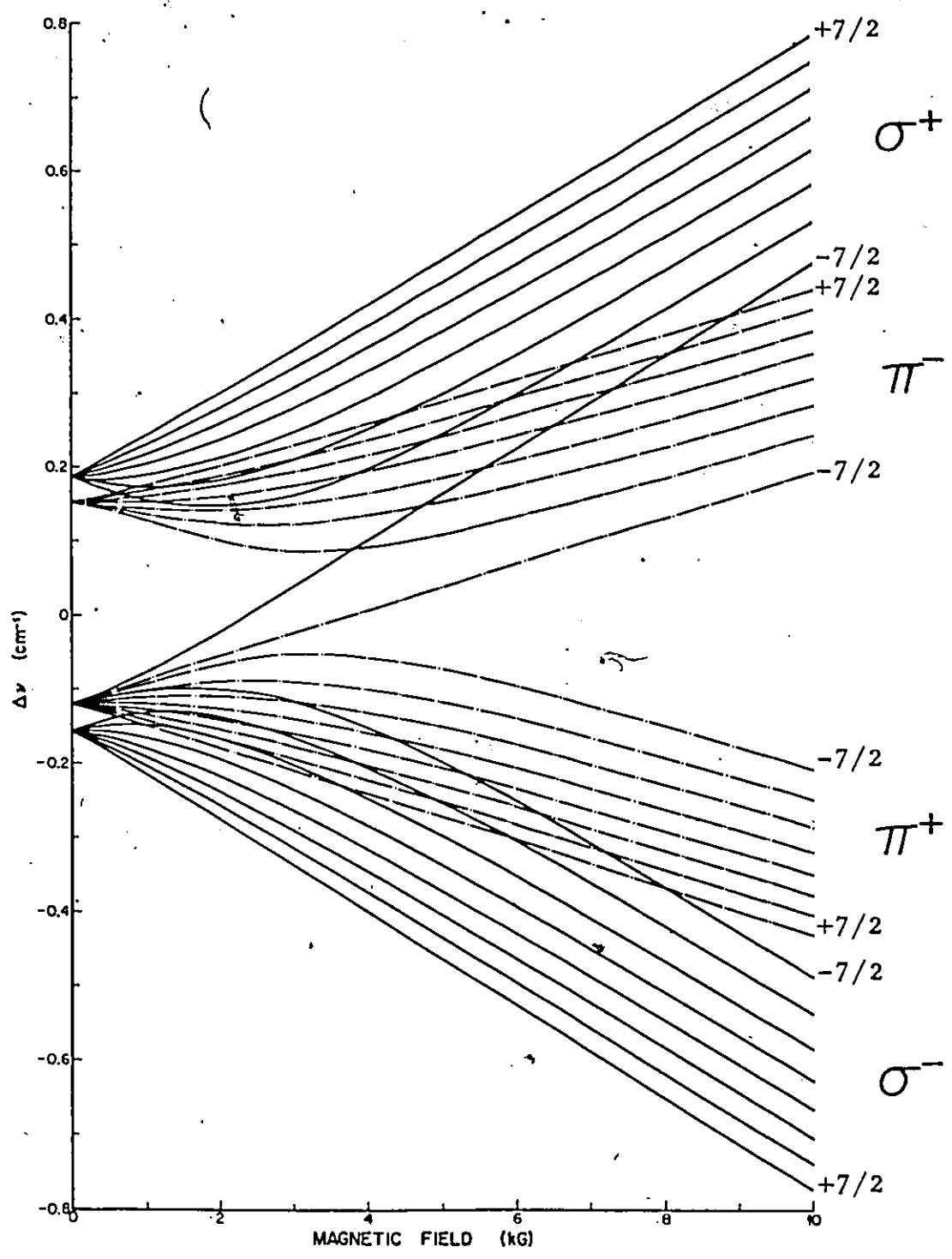
Figure 1.   The Zeeman splitting of the 8943-Å
absorption line by a magnetic field in the range 0 - 10 kG,
as calculated from the Breit-Rabi Equation (Breit and
Rabi 1931).

Figure 2.   The selective excitation of resonance
fluorescence in the Zeeman components of the $6^2P_{1/2}$ level
in cesium. (a) Coincidences between the hfs components of
the 8943-Å line emitted by the lamp and the Zeeman compo-
nents in the fluorescence cell.   The Zeeman splitting was
obtained using the Breit-Rabi Equation.   (b) Experimental
intensity profile of the fluorescence observed parallel to
the magnetic field.
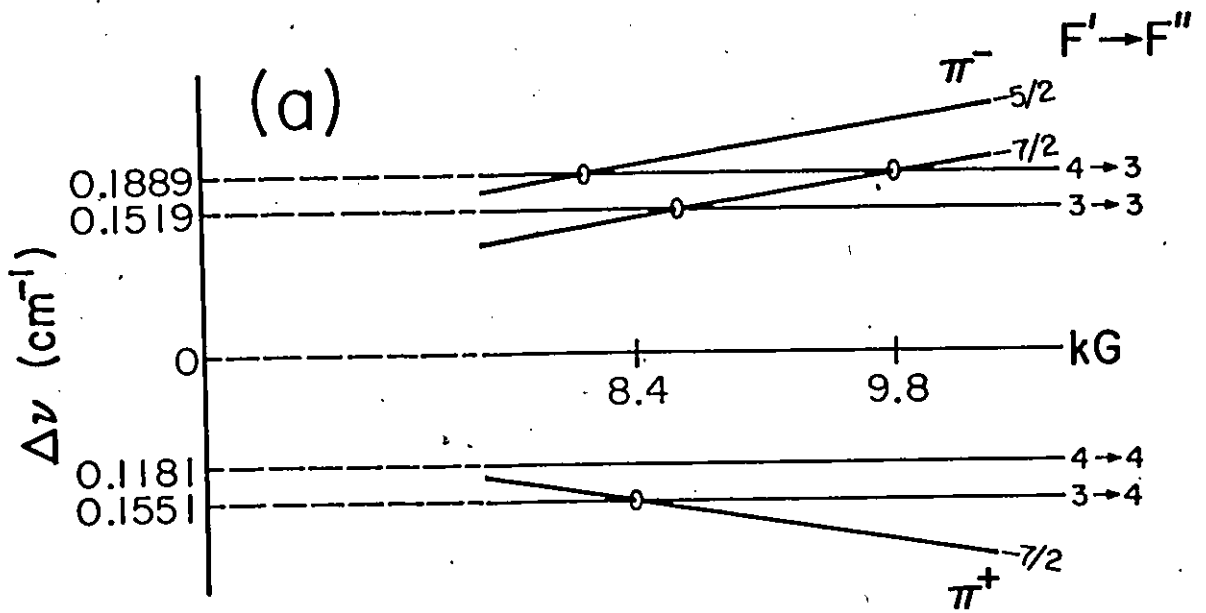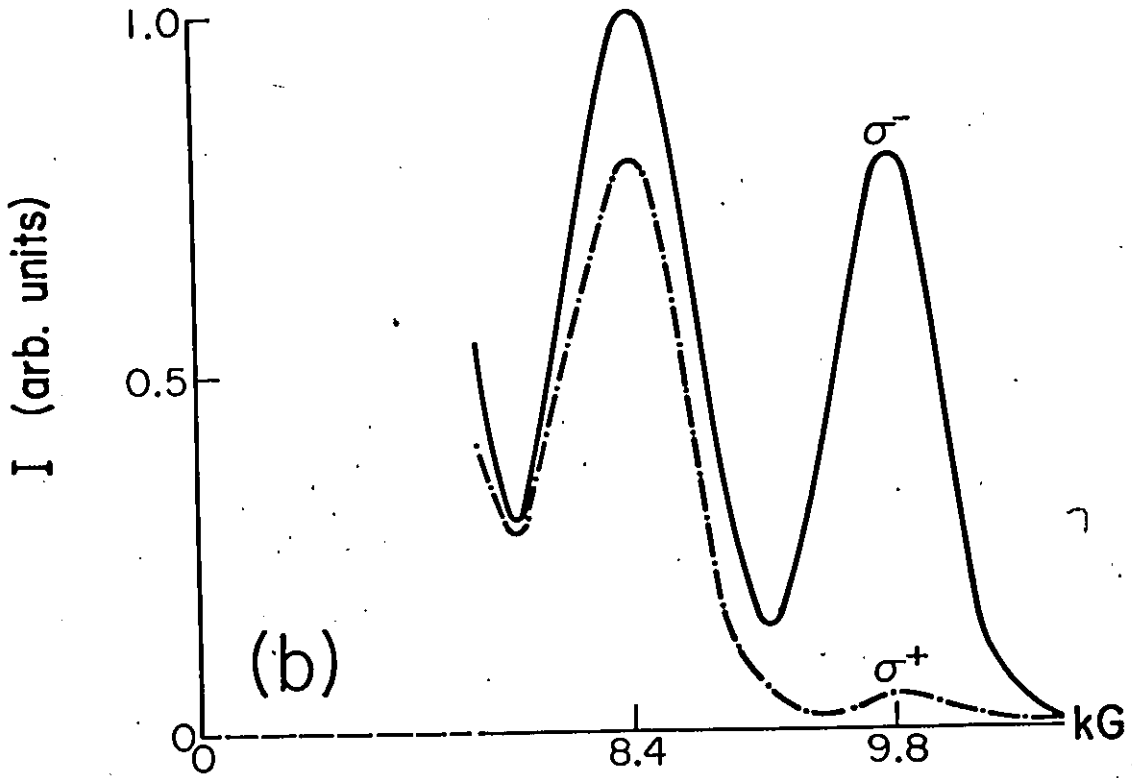
cm^{-1} hfs component coincides with the π^- (-7/2) Zeeman component. This results in the selective population of the $^2P_{\frac{1}{2}}$, $m_J=-\frac{1}{2}$, $m_I=-7/2$ sublevel. In the absence of depolarizing collisions, fluorescent light is emitted as the result of the decay of the Zeeman sublevels which had been optically excited. Thus the fluorescent light observed parallel or antiparallel to the magnetic field should be circularly polarized at a field of 9.8 kG and should be partially depolarized at magnetic fields corresponding to other coincidences shown in Figures 1 and 2. Consequently a magnetic field scan of circularly analyzed fluorescent light emitted in the direction parallel to the field produces an intensity profile shown in Figure 2(b). At 9.8 kG the polarization is virtually complete and an intense σ^- peak may be seen, accompanied by other peaks at lower fields whose positions correspond to other coincidences between the hfs components in emission and Zeeman components in absorption. The degree of circular polarization P_O may be experimentally determined in each peak by means of the relation

(II-1) $$P_O = (I_{\sigma^-} - I_{\sigma^+})/(I_{\sigma^-} + I_{\sigma^+})$$

where I_{σ^-} and I_{σ^+} are the peak intensities of the σ^- and σ^+ components respectively.

2. Excitation of the Cs $6^2P_{\frac{1}{2}}$ State in a Variable Magnetic Field with Circularly Polarized Light

In the previous section, the excitation of a single

Zeeman subststate was described, using unpolarized light incident on the fluorescing vapour in a direction perpendicular to the scanning field M_2 which was varied in the vicinity of 9.8 kG.

To make measurements possible over a wide range of M_2 values, it was necessary to alter the method of excitation and the geometry of the experiment. The spectral lamp emitting the exciting light was located in a field M_1 which was parallel to the exciting light beam. The latter was circularly polarized and made incident on the fluorescence cell in a direction approximately parallel to M_2.

As may be seen in Figure 1, it is possible to excite σ components in fluorescence over the range of field values 0 - 10 kG, provided that the exciting light is the same frequency as the absorption line. This might best be done by setting $M_1 = M_2$ for several different values of the field, because then the Zeeman splittings of the emission and absorption lines are equal and there is "maximal overlap" of the two profiles and a maximum of fluorescent intensity.

A reasonable approximation to this situation is realized by employing two different values of M_1; one relatively small and the other relatively large. The values of 0.4 kG and 8 kG were chosen. At 0.4 kG the emission line was relatively broad and intense, and free of self-reversal, which permitted fluorescence measurements to be carried out in the M_2 range 0 - 6.5 kG. 8 kG was the largest field

which could be employed within the limitations of the M_1 power supply, and permitted measurements in the vicinity of $M_2=8$ kG. As the magnitude of M_2 is increased, various coincidences between the Zeeman lines in emission and absorption result in continuous excitation of the $6^2P_{\frac{1}{2}}$ level, subject to the selection rule $\Delta m=+1$. Figure 3 shows the σ^+ and σ^- profiles resulting from an M_2 scan from 0 to 10 kG, with M_1 fixed at 0.4 kG, using σ^+ excitation and monitoring separately the σ^+ and σ^- components. The diminished fluorescent intensity which is observed as M_2 approaches 10 kG, was comparable to the level of the non-fluorescent background signal and served as the zero reference level for the fluorescent intensity. As should be expected, both profiles exhibit a maximum in the vicinity of 0.4 kG and slowly decrease as M_2 is increased. Figure 4 shows the profile of the intensity differences $(I_{\sigma^+} - I_{\sigma^-})$ for $M_1=8$ kG, showing a distinct intensity maximum in the vicinity of $M_2=8$ kG. The intensity sum $(I_{\sigma^+} + I_{\sigma^-})$ was also recorded and the diminished intensity level at $M_2=0$ was used to determine the level of the non-fluorescent signal.

3. Excitation of the Cs $6^2P_{3/2}$ State in a Variable Magnetic Field with Polarized Light

(a) Excitation With Circularly Polarized Radiation

The Zeeman pattern of the Cs 8521-Å resonance line arising from the transition $6^2P_{3/2}-6^2S_{\frac{1}{2}}$, is more complex than that of the 8943-Å $(6^2P_{\frac{1}{2}}-6^2S_{\frac{1}{2}})$ line because of a larger

Figure 3.   Traces of magnetic field scans of the 8943-Å fluorescence observed parallel to the magnetic field with the spectral lamp located in a 0.4 kG magnetic field.
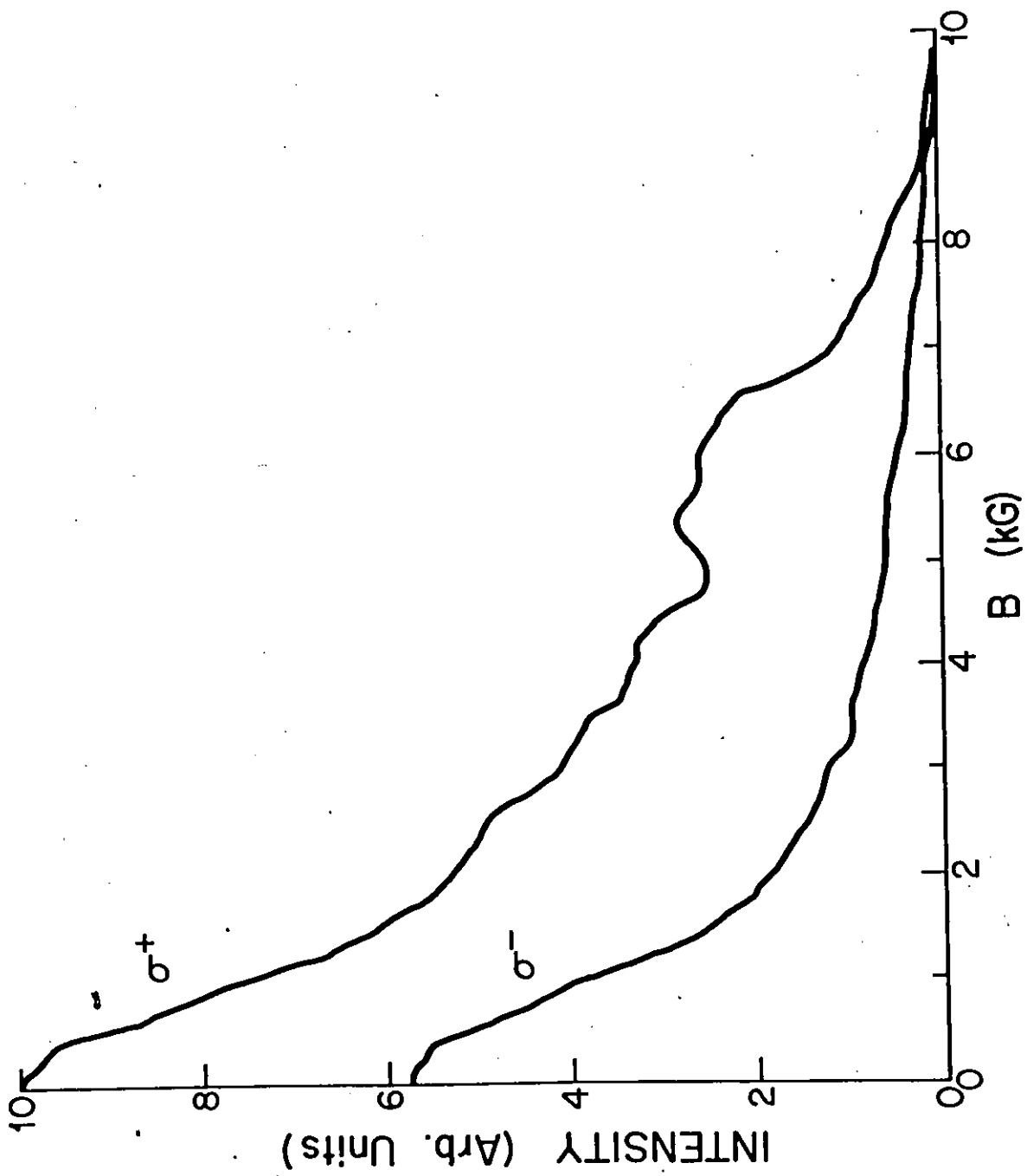
Figure 4.   Traces of magnetic field scans of the 8943-Å Fluorescence signal $(I_{\sigma^+} - I_{\sigma^-})$ at 0 torr and 3.92 torr He with the spectral lamp in an 8 kG magnetic field.

INTENSITY (Arb. Units)

B (kG)

0.00 Torr He

3.92 Torr He
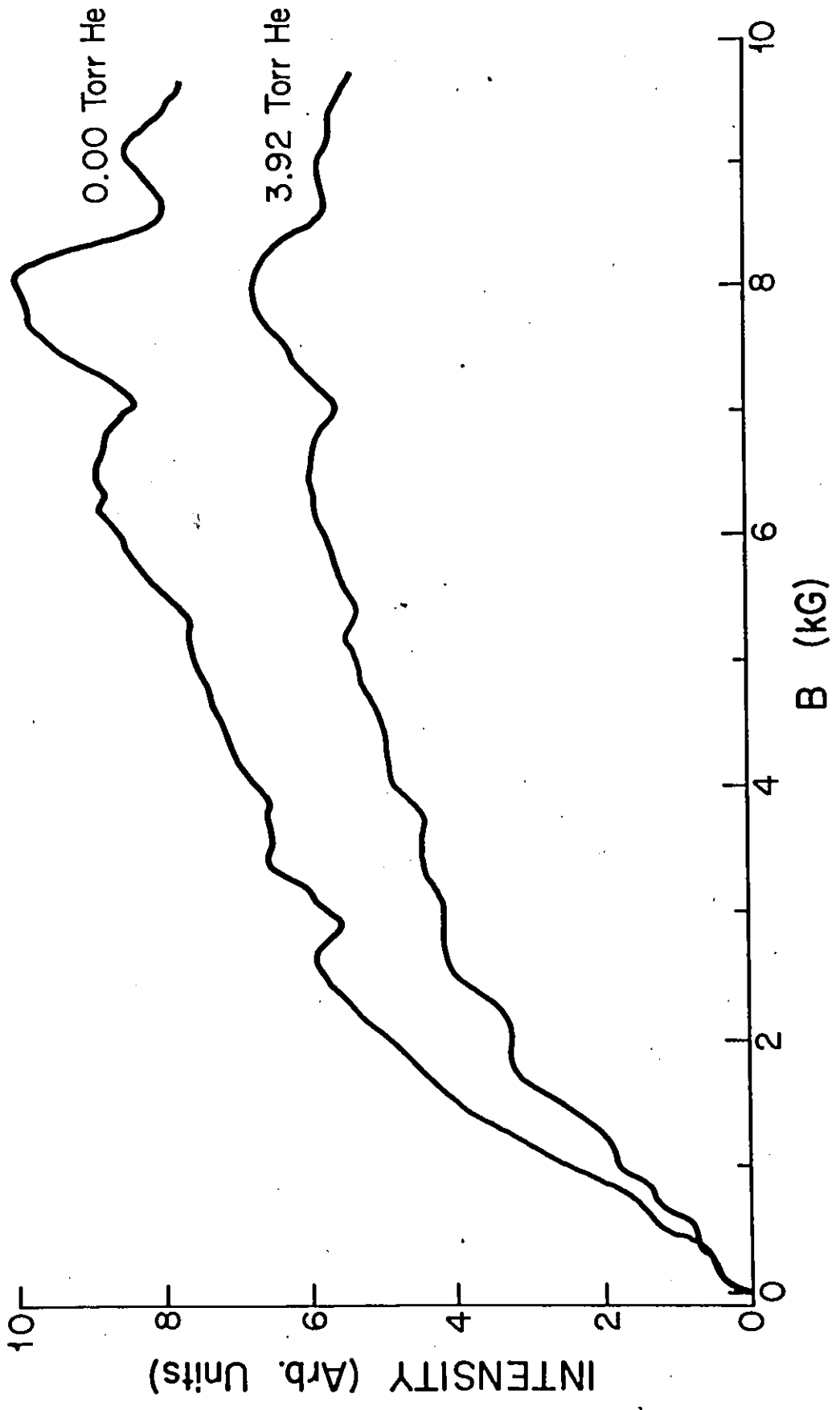
number of sublevels. The Breit-Rabi formula cannot be applied in the case of $^2P_{3/2}$ levels (Breit and Rabi 1931) but it does provide, at least, a qualitative description of the Zeeman structure, which agrees with experimentally obtained intensity profiles. For the case of broad line excitation with $M_1 = 0.4$ kG, and circularly polarized light incident parallel to M_2, the intensity profiles shown in Figure 5 have peaks in the vicinity of 0.4 kG, and exhibit low and broad maxima centred near 5 kG. The maxima at 5 kG arise from the excitation of the m_I manifold associated with the $m_J = +3/2$ Zeeman sublevel. At higher M_2 field strengths, the intensity decreases so that in the vicinity of 10 kG, the signal is indistinguishable from the background.

(b) Excitation With Linearly Polarized Radiation

When linearly polarized resonance radiation is used to excite the Cs $6^2P_{3/2}$ state, the transitions take place according to the selection rule $\Delta m_F = 0$ and the resulting resonance fluorescence is also linearly polarized. The axis of quantization is defined by the direction of the electric vector of the exciting light beam. The magnetic field M_2 was then applied in the direction parallel to the exciting light beam. As expected, it was found that the resonance fluorescence retained a degree of linear polarization only at very low fields, as at higher fields the rapid precession of the atomic dipole in the field results in complete depolarization. The fluorescent intensity profiles obtained with linearly polarized exciting light are shown in Figure 6;

Figure 5. Traces of magnetic field scans of circularly polarized 8521-Å fluorescence observed parallel to the magnetic field. The spectral lamp was located in 0.4 kG field and σ^+ light was used for excitation.
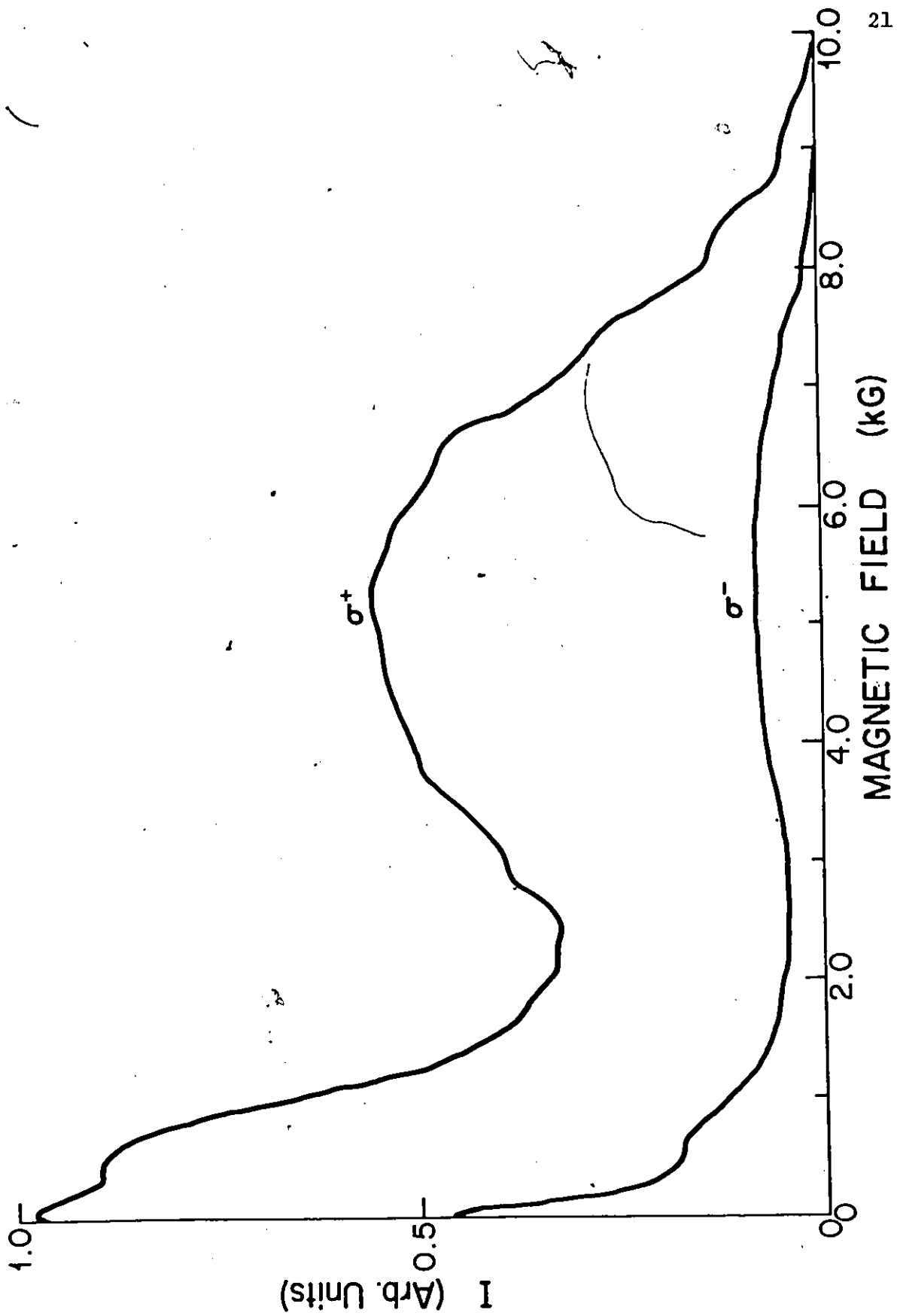
Figure 6. Traces of magnetic field scans of linearly polarized 8521-Å fluorescence observed parallel to the magnetic field. The spectral lamp was located in 0.4 kG field and π^+ light was used for excitation.
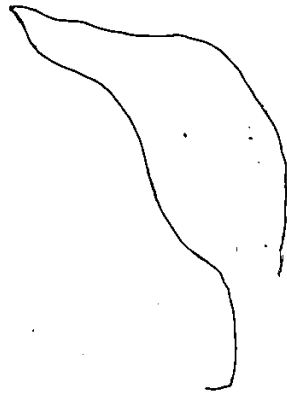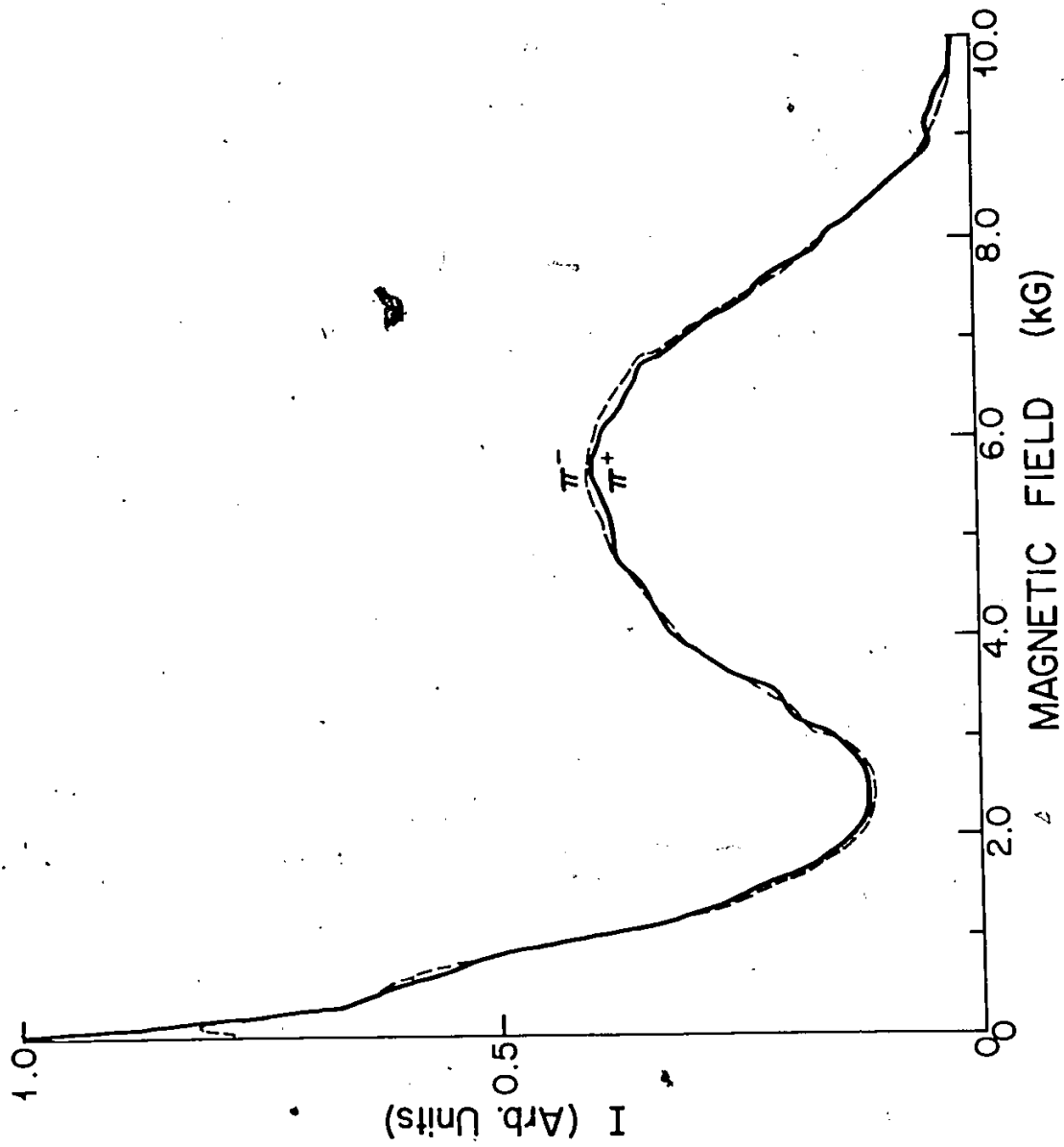
their overall shapes are similar to those in Figure 5 except
near zero field.

III. THEORY OF COLLISIONAL DEPOLARIZATION

1. Disorientation of $6^2P_{\frac{1}{2}}$ Cs Atoms in Collisions with Noble Gases.

When cesium atoms in mixture with a buffer gas are continuously excited with circularly polarized light to one m_J sublevel of the $6^2P_{\frac{1}{2}}$ state, they become oriented with respect to the axis of the light beam. The orientation is destroyed through spontaneous decay and m_J mixing collisions with the buffer gas atoms. The resulting quasi-equilibrium value for the orientation, $\langle J_z \rangle_e^{eq*}$ is given by the following expression which takes no account of nuclear spin.

(III-1) $$\langle J_z \rangle_e^{eq} = 1/2 \ [1/(1+Z\tau)]$$

which is equivalent to the Stern-Volmer equation (Stern and Volmer 1919)

(III-2) $$P = 1/(1+Z\tau)$$

In the absence of depolarizing collisions and under ideal experimental conditions, the measured degree of polarization should be equal to unity. The departure from ideal conditions is compensated by a correction factor P_o which is introduced into Equation (III-2), resulting in

(III-3) $$P = P_o/(1+\tau Z)$$

* $\langle J_z \rangle_e^{eq}$ is the quasi-equilibrium value for the orientation, Z is the frequency of disorienting collisions per $^2P_{1/2}$ atom, τ is the lifetime of the Cs $^2P_{1/2}$ state $(3.4 \times 10^{-8}$ sec) and P is the polarization.

Equation (III-3) provides the connection between the experimentally determined degree of polarization and the thermally averaged disorientation cross section Q which is defined analogously with the gas-kinetic cross section

(III-4) $$Z = n \, v_r \, Q$$

where n is the density of buffer gas atoms and v_r is the average relative speed of the colliding partners.

Equation (III-2) makes no provision for the effect of the nuclear spin on the relaxation process, which can be important at low magnetic fields. It is well known that; when the experimental determination is based on the Hanle effect, failure to consider the effects of nuclear spin may lead to differences of several hundred per cent between the measured and true cross sections. However, the effect of nuclear spin on depolarization experiments is much less pronounced and differences between the actual and measured values amount to less than 25%.

Franz and Sooriamoorthi (1973) recognized the importance of this effect and derived quasi-equilibrium values for $\langle J_z \rangle_e^{eq}$, corresponding to various values of I. For $^2P_{1/2}$ Cs atoms (I=7/2):

(III-5) $$\langle J_z \rangle_e^{eq} = 1/2 \, (11 + Z\tau) \, [(1 + Z\tau)(32 + Z\tau)]^{-1}$$

or, in terms of the polarization,

(III-6) $P = P_O (11 + Z\tau) [(1 + Z\tau)(32 + Z\tau)]^{-1}$.

Under ideal conditions ($P_O=1$) and in the absence of disorienting collisions, Equation (III-6) becomes

(III-7) $P = \frac{11}{32} = 0.344$

Eq. (III-2), on the other hand, yields

$P = 1.0$.

Franz and Sooriamoorthi assumed in their treatment, which applies to the case of zero magnetic field, that the optical pumping is weak and that the collision frequencies are lower than the $^2P_{\frac{1}{2}}$ hyperfine frequency. These criteria were fulfilled in the present investigation by using a low-power spectral lamp and restricting buffer gas pressures to less than 10 torr.

Figure 7 shows curves for I=0, 3/2, and 7/2 (Sooria-moorthi 1974) of the normalized equilibrium orientation $\alpha \langle J_z \rangle_e^{eq}$ plotted against $\Gamma_1 \tau$, where α is a normalizing factor different for each I, and Γ_1 is the collisional relaxation rate for the orientation. For values of $\Gamma_1 \tau$ greater than 1.5, the depolarization rate corresponding to I=3/2 is approximately 20% lower than for I=0 and in the case of I=7/2, it is approximately 5% lower. Under the conditions of this experiment, the maximum value of $\Gamma_1 \tau$ was less than 0.2 for

Figure 7.   The dependence of the normalized

values of $\langle J_z \rangle_e^{eq}$ for the $^2P_{1/2}$ state, on the degree of

collisional relaxation $\Gamma_1 \tau$, for nuclear spin $\vec{I} = 0$, $3/2$,

and $7/2$.
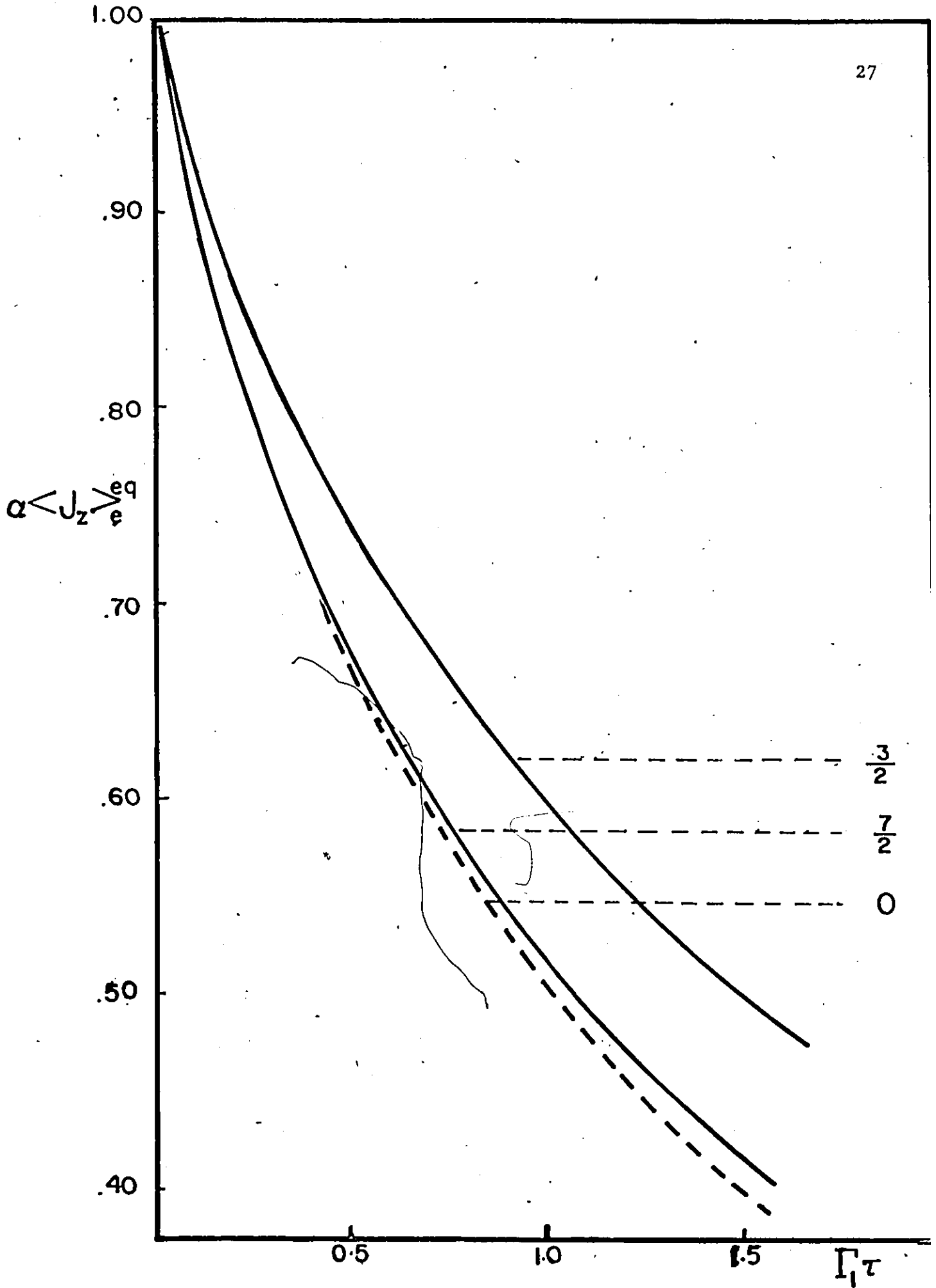
which the disorientation rates for I=7/2 and I=0 are indistinguishable. Thus, in the present investigation, the Stern-Volmer equation can be used for the analysis of the depolarization data, even at zero magnetic field. Nevertheless, data obtained in the vicinity of zero field were analyzed using both Equations (III-6) and (III-3), but for the results obtained at high magnetic fields, the Stern-Volmer equation was used. A detailed analysis of the various processes involving the populations of specific Zeeman sublevels would be tedious, in view of the complexities involved. Such an analysis is not required in this instance, especially in view of the validity of the nuclear decoupling approximation on which Equation (III-6) is partly based.

In the particular instance when a single Zeeman sublevel $m_J = -\frac{1}{2}$, $m_I = -7/2$, is excited in magnetic fields sufficiently large to produce the Back-Goudsmit effect, the following equation describes the depolarization induced by collisions with ground-state noble gas atoms.

(III-8) $Cs \ (6^2P_{1/2}, \ m_J = -1/2, \ m_I = -7/2) + X(^1S_0) + \Delta E$

$\rightleftharpoons Cs \ (6^2P_{1/2}, \ m_J = +1/2, \ m_I = -7/2) + X(^1S_0),$
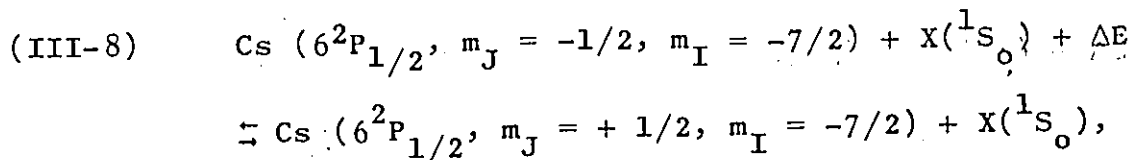
where $X(^1S_0)$ is a noble-gas atom in its ground state and ΔE is the energy defect between the $m_J = -\frac{1}{2}$, $m_I = -7/2$ and $m_J = +\frac{1}{2}$, $m_I = -7/2$ substates. It is assumed that m_I remains unchanged during the collision.

The vapour-gas mixture is considered to be in a

state of dynamic equilibrium which involves the continuous excitation of cesium atoms to the $m_J=-\frac{1}{2}$, $m_I=-7/2$ Zeeman sublevel of the $6^2P_{\frac{1}{2}}$ state, spontaneous decay, and inelastic collisions. The equilibrium may be represented by the following rate equations (See Figure 8):

(III-9) $\quad \dfrac{dn(-)}{dt} = \dfrac{-n(-)}{\tau} - Z(-)n(-) + Z(+)n(+) + s(-) = 0$

(III-10) $\quad \dfrac{dn(+)}{dt} = \dfrac{-n(+)}{\tau} - Z(+)n(+) + Z(-)n(-) = 0$

where $\tau=3.4\times10^{-8}$ sec. is the average lifetime of the $6^2P_{\frac{1}{2}}$ state, (Link 1966) $n(-)$ and $n(+)$ are the densities of the atoms in the $m_J=-\frac{1}{2}$, $m_I=-7/2$ and $m_J=+\frac{1}{2}$, $m_I=-7/2$ substates, $Z(-)$ and $Z(+)$ are the collision numbers corresponding to the $m_J=-1/2$, $m_I=-7/2 \rightarrow m_J=+1/2, m_I=-7/2$ and $m_J=+1/2$, $m_I=-7/2 \rightarrow m_J=-1/2$, $m_I=-7/2$ transitions, respectively, between the Zeeman sublevels of the $^2P_{1/2}$ state, and $s(-)$ is the density of atoms excited per second to the $6^2P_{1/2}$, $m_J=-1/2$, $m_I=-7/2$ substate. Equations (III-9) and (III-10) may be solved to give the ratio of the atomic densities:

(III-11) $\quad n(+)/n(-) = Z(-)/[Z(+) + 1/\tau]$

The degree of circular polarization P is defined in terms of the intensities of the σ^- and σ^+ components:

(III-12) $\quad P = (I_{\sigma^-} - I_{\sigma^+})/(I_{\sigma^-} + I_{\sigma^+})$

Figure 8.   Radiative and collisional transitions
between the Zeeman sublevels of the $6^2S_{1/2}$ and $6^2P_{1/2}$
states.   Broken arrows indicate decays not observed in
the experiment.
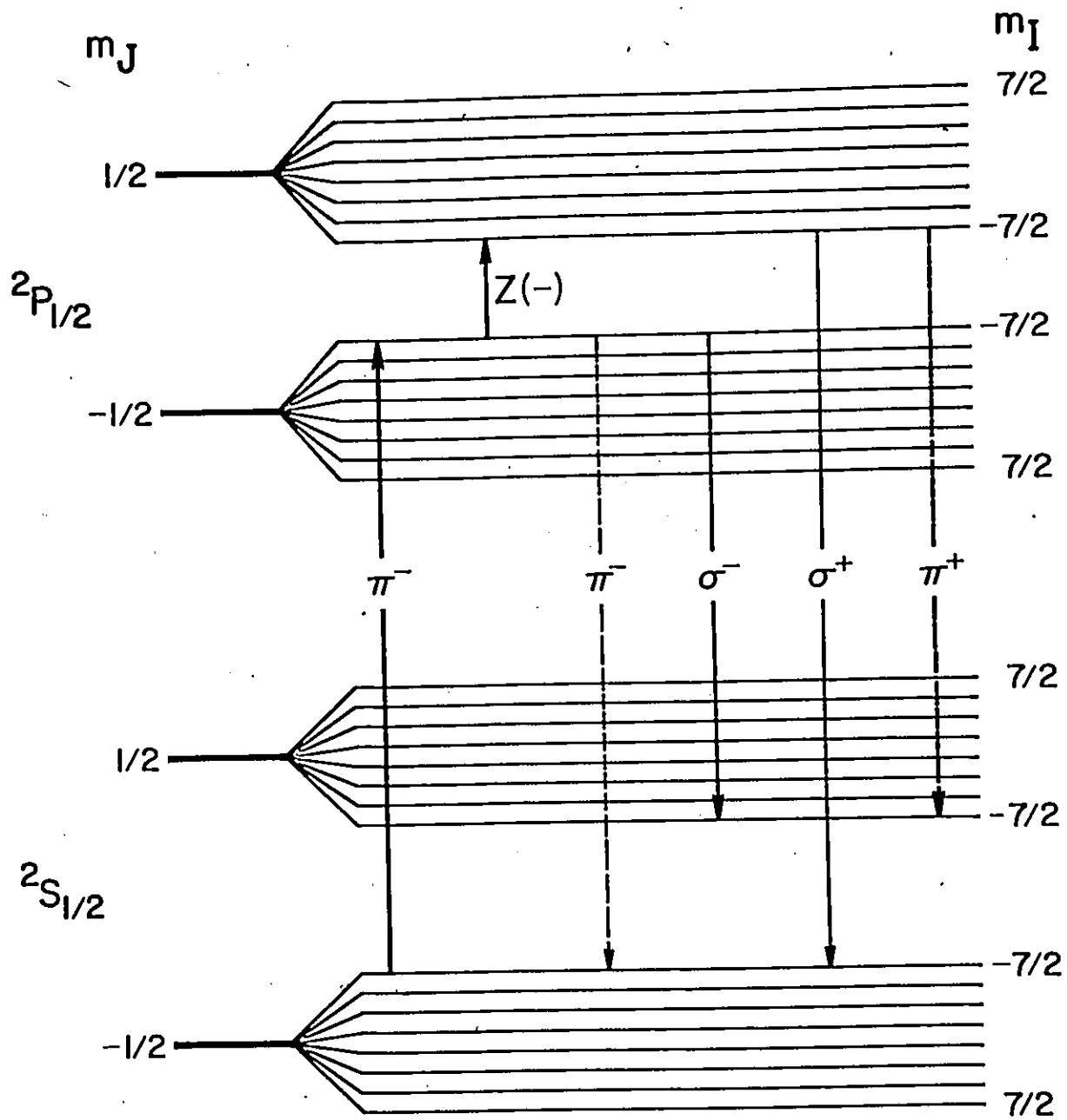
The transition probabilities of the σ^- and σ^+ transitions are equal to one another and, consequently,

(III-13) $\quad I_{\sigma^-} = An(-)$, and $I_{\sigma^+} = An(+)$

where A is proportional to the Einstein A coefficient. Equations (III-12) and (III-13) yield

(III-14) $\quad P = (1-\frac{n(+)}{n(-)})/(1+\frac{n(+)}{n(-)})$

The combination of Equations (III-11) and (III-14) establishes the relationship between the collision numbers $Z(+)$ and $Z(-)$ and the degree of polarization P:

(III-15) $\quad P = \dfrac{Z(+) + 1/\tau - Z(-)}{Z(-) + Z(+) + 1/\tau}$

According to the principle of detailed balancing, $Z(+)=Z(-)$, because the statistical weights of the two Zeeman substates are equal to one another and the energy separation between the substates is negligible compared with kT. Thus Equation (III-15) reduces to the Stern-Volmer Equation (See Equation (III-2).), in which $Z=Z(+)+Z(-)$. It has been assumed that the influence of collisional mixing between the $^2P_{\frac{1}{2}}$ and $^2P_{3/2}$ fine structure states on the polarization is negligible.

2. Collisional Disorientation and Disalignment of $6^2P_{3/2}$ Cs Atoms

The results of an experiment, in which the Cs $6^2P_{3/2}$ state is excited with polarized light in a weak magnetic field, and the polarization of the resonance fluorescence resulting from its spontaneous decay is monitored in relation to the buffer gas pressure, may be analyzed using the Stern-Volmer relation, as given in Equation (III-3), bearing in mind that $\tau=30.5$ ns is the lifetime of the $6^2P_{3/2}$ state (Link 1966). A least-squares fit of Equation (III-3) to an experimental plot of the degree of polarization against noble gas density, yields the depolarization cross section if it is assumed that collisional fine-structure mixing may be neglected. When the polarization of the exciting and fluorescent light is circular or linear, Q represents the cross section Q(circ.) for circular depolarization, or Q(lin.) for linear depolarization, which, in the absence of nuclear spin, would be representative of the disorientation and disalignment cross sections, respectively.

When the fluorescence is excited in a magnetic field above 5 kG, which completely decouples the nuclear spin, the cross section for circular depolarization is identical with the cross section for disorientation of the $^2P_{3/2}$ state, provided that the field is also sufficiently strong to separate the various m_J Zeeman substates, so that only those energy levels associated with a single m_J value become excited. Figure 9 shows the various radiative and collisional processes that are involved in the establishment of the steady state which is assumed to exist under the condi-

Figure 9.   Radiative and collisional transitions

between the Zeeman sublevels of the $6^2S_{1/2}$ and $6^2P_{3/2}$

states, involved in circular depolarization.   The unresolved

hfs is indicated by the dotted regions.
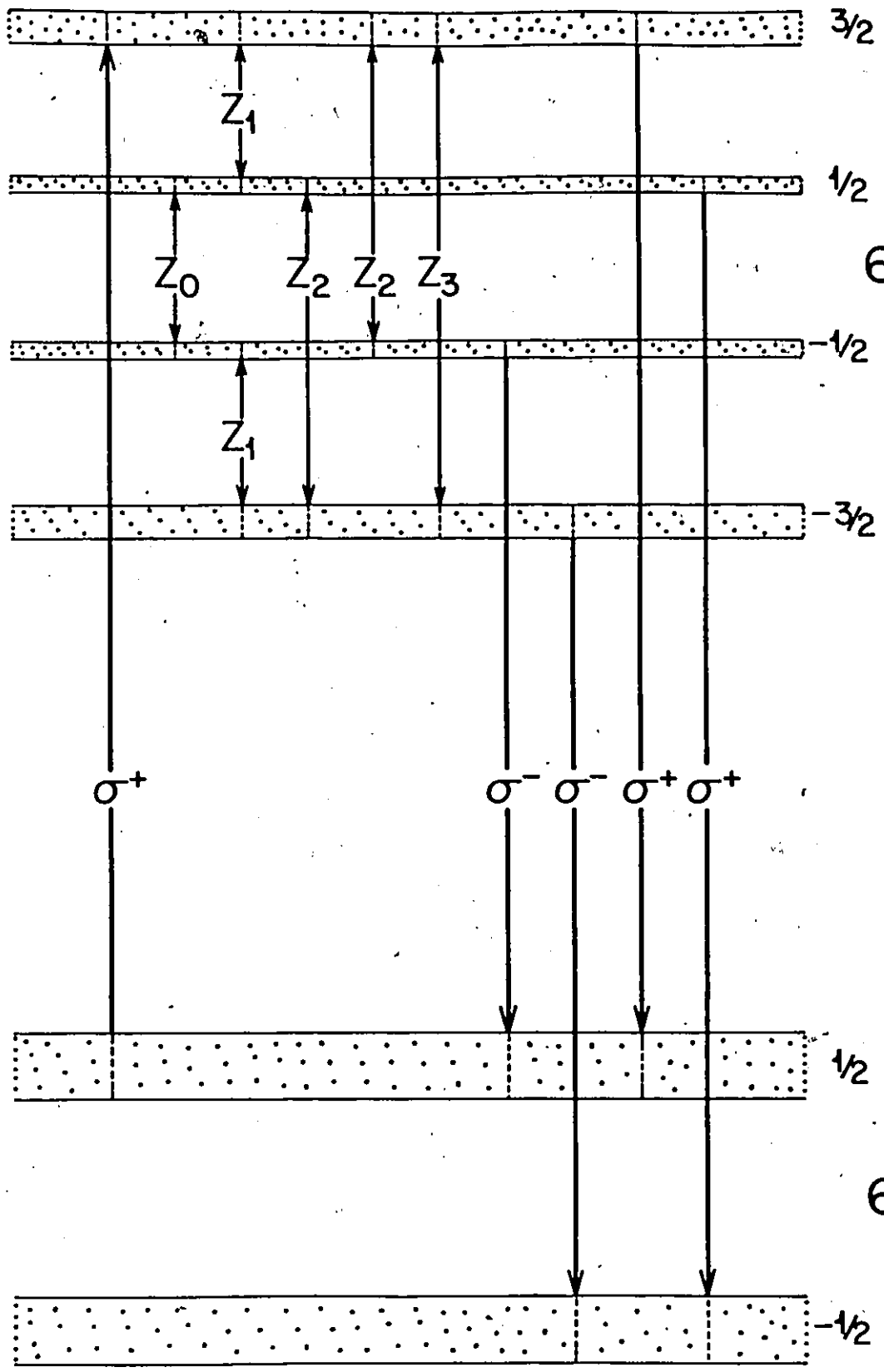
tions of the experiment. Because of broad-line excitation, transitions between individual $\dot{m}_I$ states are not resolved and, in any case, distinctions between m_I states with respect to particular collisional transitions are unimportant, since the nuclear orientation remains unaffected during a collision. Consequently, each m_J level in Figure 9 is indicated by a broad band which represents all the associated m_I components. The dynamic equilibrium which results from the processes of optical excitation, spontaneous decay and collisional m_J mixing, may be represented by the following rate equations which are identical with those applicable to the case of the $4^2P_{3/2}$ state in potassium (Berdowski et al. 1971).

(III-16)
$$\frac{dn_{-3/2}}{dt} = \frac{-1}{\tau} n_{-3/2} - Z_1 n_{-3/2} - Z_2 n_{-3/2} - Z_3 n_{-3/2}$$
$$+ Z_1 n_{-1/2} + Z_2 n_{1/2} + Z_3 n_{3/2} + s_{-3/2} \Big\} = 0$$

(III-17)
$$\frac{dn_{-1/2}}{dt} = \frac{-1}{\tau} n_{-1/2} - Z_1 n_{-1/2} - Z_o n_{-1/2} - Z_2 n_{-1/2}$$
$$+ Z_1 n_{-3/2} + Z_o n_{1/2} + Z_2 n_{3/2} + s_{-1/2} = 0$$

(III-18)
$$\frac{dn_{1/2}}{dt} = \frac{-1}{\tau} n_{1/2} - Z_1 n_{1/2} - Z_o n_{1/2} - Z_2 n_{1/2}$$
$$+ Z_1 n_{3/2} + Z_o n_{-1/2} + Z_2 n_{-3/2} + s_{1/2} = 0$$

(III-19)
$$\frac{dn_{3/2}}{dt} = \frac{-1}{\tau} n_{3/2} - Z_1 n_{3/2} - Z_2 n_{3/2} - Z_3 n_{3/2}$$
$$+ Z_1 n_{1/2} + Z_2 n_{-1/2} + Z_3 n_{-3/2} + s_{3/2} = 0$$

where $\tau = 30.5$ ns is the lifetime of the $^2P_{3/2}$ state (Link 1966), $n_{-3/2}$, $n_{-1/2}$, $n_{1/2}$ and $n_{3/2}$ are the densities of $6^2P_{3/2}$ cesium atoms in the $m_J=-3/2$, $-1/2$, $1/2$ and $3/2$ substates, respectively, and Z_0, Z_1, Z_2 and Z_3 are the frequencies of collisions per excited cesium atom, corresponding to the following transitions between the Zeeman substates of the $6^2P_{3/2}$ state, respectively: $-\frac{1}{2} \leftrightarrow +\frac{1}{2}$, $\mp\frac{3}{2} \leftrightarrow \mp\frac{1}{2}$, $\mp\frac{3}{2} \leftrightarrow \pm\frac{1}{2}$ and $-\frac{3}{2} \leftrightarrow +\frac{3}{2}$; the collision numbers Z_n are connected as follows with the corresponding cross sections:

(III-20) $Z_i = n Q_i v_r$

$s_{-3/2}$, $s_{-1/2}$, $s_{1/2}$ and $s_{3/2}$ are the densities of $^2P_{3/2}$ cesium atoms, excited optically per second to the $m_J=-3/2$, $-1/2$, $1/2$ and $3/2$ substates, respectively. Equations (III-16) - (III-19) become simplified if only the $m_J=+3/2$ state is excited optically (as was the case in this investigation). The use of an argument analogous to that employed by Berdowski et al. (1971), leads to the following expression for the polarization of the fluorescence.

(III-21) $P = P_o 3(1 + \tau\gamma_2)/(1 + \tau\gamma_1)(3 + 2\tau\gamma_2)$,

where γ_1 and γ_2 are the collisional decay rates of orienta-
tion and alignment, respectively (D'yakonov and Perel' 1965),
which may be expressed as follows in terms of the corresponding
cross sections.

(III-22) $\qquad \gamma_i = N\sigma_i v_r$

An analysis of experimental depolarization data
obtained at high magnetic fields, carried out with the aid of
Equations (III-21) and (III-22), yields the cross sections for
collisional disorientation and disalignment of the $6^2P_{3/2}$
cesium atoms.

It should be borne in mind that the collisional
relaxation of circular or linear polarization in the presence
of atomic hyperfine structure, involves all the multipole
relaxation rates γ_i, but is dominated by γ_1 in the case of
circular polarization and γ_2 for linear polarization. When
$I = 0$ or when the nuclear spin is completely decoupled in
a strong field $Q(\text{circ.}) \equiv \sigma_1$ and $Q(\text{lin.}) \equiv \sigma_2$ (Rebane and
Rebane 1972)*.

---

* These authors employ the concept of 'Born polarization'
  which differs from the degree of polarizations as defined
  in Eqs. (II-1) and (V-2) (Rebane et al. 1972).

IV.   EXPERIMENTAL

1.   Description of the Apparatus

Figure 10 shows a block diagram of the apparatus employed to study the collisional disorientation of $6^2P_{\frac{1}{2}}$ Cs atoms at a fixed field M_2 of 9.8 kG, and using unpolarized light for excitation.

Light from a cesium rf lamp was passed through an 8943-Å interference filter and was brought to a focus in the fluorescence cell which contained cesium vapour at a pressure of 10^{-6} torr, mixed with a noble gas; the cell was mounted between the pole pieces of the electromagnet. The fluorescent light was observed along the magnetic field axis through an aperture in the pole piece and was focused onto the photocathode of a cooled photomultiplier. The output of the latter was amplified and applied to the Y axis of the X - Y recorder, to whose X axis was applied the output of a gaussmeter which monitored the strength of the field. The inclusion of circular analyzers in the fluorescent light beam permitted the separate observation of the σ^- and σ^+ components and the direct recording of their intensities in relation to the magnetic field.

The arrangement of the apparatus for the study of collisional depolarization of the $6^2P_{\frac{1}{2}}$ and $6^2P_{3/2}$ cesium atoms in variable magnetic fields, and using polarized light for excitation, is shown in Figure 11. The spectral lamp was located in the magnetic field M_1 and the cesium resonance

37

Figure 10. The arrangement of the apparatus used to study depolarization of Cs $^2P_{1/2}$ atoms, employing excitation with unpolarized 8943-Å radiation directed perpendicular to the magnetic field (M – magnet; C – fluorescence cell; PM – photo-multiplier; E – electrometer; R–X–Y plotter; G – gaussmeter; F – interference filters; $\lambda/4$ – quarter wave plates; P – polaroids).
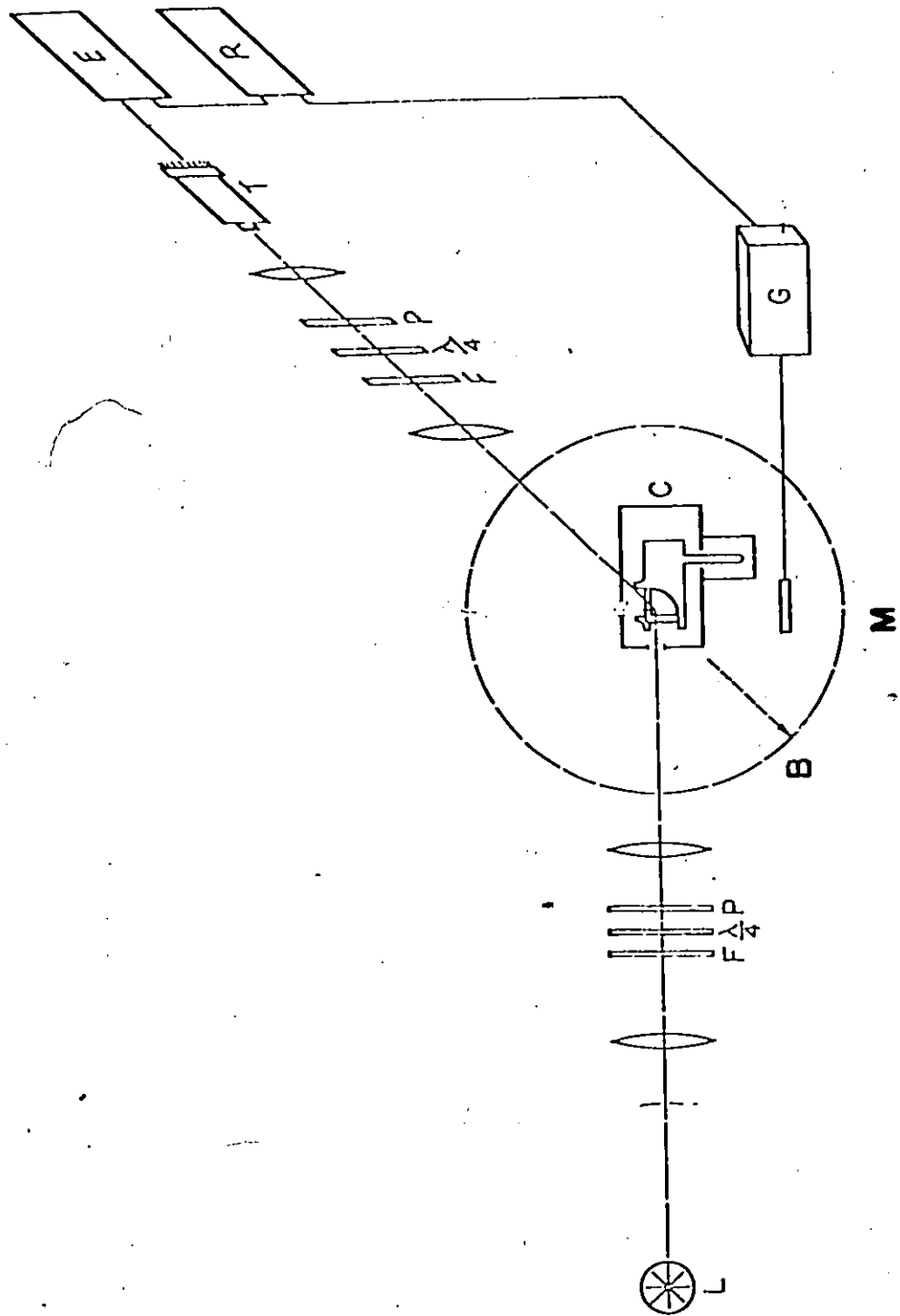
Figure 11. The arrangement of the apparatus used to study depolarization of $^2P_{1/2}$ and $^2P_{3/2}$ Cs atoms, employing excitation with polarized resonance radiation directed parallel to the magnetic field (L - lamp; M_1, M_2 - electromagnets; C - fluorescence cell; G - gaussmeter; PM - photomultiplier; E - electrometer; R-X-Y plotter; F - interference filter; $\lambda/4$ - quarter wave plates; P - polaroids).

radiation emitted from it was passed through appropriate interference filters and polarizers (circular or linear), and was brought to a focus in the fluorescence cell which contained Cs vapour at low pressure. The cell was mounted between the poles of magnet M_2 which generated a magnetic field parallel to the exciting light beam.

In the investigation of the $6^2P_{\frac{1}{2}}$ Cs atoms, σ^+-polarized resonance radiation of wavelength $8943\text{-}\overset{o}{A}$ was used for excitation. The resonance fluorescence was observed along the direction of the magnetic field through the aperture in the pole piece. Inclusion of circular analyzers in the fluorescent light beam permitted the separate observation of the σ^+ and σ^- components of the fluorescence, the intensities of which were recorded in relation to the M_2 magnetic field strength.

The Cs $^2P_{3/2}$ atoms can undergo collisional disalignment as well as disorientation, each of which was studied separately. In the experiments dealing with disorientation, σ^+-polarized $8521\text{-}\overset{o}{A}$ radiation was used for excitation and the resulting fluorescence was analyzed with respect to circular polarization. The study of disalignment at zero magnetic field (destruction of linear polarization) involved excitation with linearly polarized $8521\text{-}\overset{o}{A}$ resonance radiation and analysis of the fluorescence with respect to linear polarization.

(a) The Spectral Lamps

The rf light source was of the electrodeless discharge type described elsewhere (Atkinson et al. 1965). The cylindrical pyrex bulb, approximately 9 cm in length and 2 cm in diameter, was tapered at one end to form a reservoir containing approximately 0.5 g of cesium metal, and was mounted vertically in the tank coil of a push-pull rf oscillator. The reservoir at the bottom of the bulb was placed in a small heater, whose temperature controlled the vapour pressure of the metal in the bulb. The oscillator was operated at a typical frequency of 83 mHz which depended on the tank coil dimensions and could be adjusted slightly by mechanical manipulation of the windings. The discharge was carried by argon whose pressures in the bulb ranged from 0.6 to 2 torr, depending on the particular bulb. When the system was operating under optimal conditions, the lamp emitted Cs resonance lines of high intensity, small half-width and no self-reversal (Atkinson et al. 1965). The intensity was stable to within 1-2% during a typical working period of 12-15 hrs.

When exciting cesium fluorescence with polarized light, the light source itself was placed in a magnetic field. This posed special problems for the design of the discharge lamp which had to be modified to make the lamp operational in a magnetic field (Berdowski et al. 1967). The pyrex bulb was in the form of a horizontal cylinder, approximately 3 cm in length and 2.5 cm in diameter, with plane windows sealing both ends and its axis along the direction of the field.

The lamp had a 2.5 cm long vertical side-arm, which contained approximately 0.5 g Cs metal and was located midway between the ends of the cylinder. The bulb, which contained 1.7 torr Ar, was mounted with its side-arm in the oscillator tank coil, and resting in a small heater. A small rectangular box, made of copper foil, with an aperture on one side, served as an rf shield of the lamp assembly. The aperture (2 cm in diameter) was combined with a second movable 3 mm aperture, which served to select the emitted radiation from a portion of the luminous discharge ring. In this way the radiation source was reduced in size and was restricted to regions of maximal intensity. The oscillator coil was connected to the oscillator by a properly matched transmission line, enabling the oscillator to be placed outside the magnetic field, and avoiding interference as well as capacitive power losses. The exciting coil was connected to the tuned coil by coaxial cables, with impedances matched to the oscillator. The cables were 170 cm long, which at 33 mHz corresponded to approximately $\lambda/4$.

(b) The Electromagnets

The two magnetic fields M_1 and M_2 were produced by Magnion Model L-128A 12 in. water-cooled electromagnets with 4 in. gaps, mounted on wheeled carriages. Their low impedance coils (1Ω) were mounted in the yoke (which was inclined at 45° to permit easy access to the field region) by means of three pins which were also used to align the

pole caps. The latter had central apertures 2 cm in diameter which permitted the observation of fluorescence in directions parallel to the magnetic field. The homogeneity of the field was better than 0.1% over the central 1 in.^{3} region. In addition, a set of coils, each consisting of 320 windings of #14 wire, was mounted on the pole caps of magnet M_2, to extend its maximal field to 10.8 kG. The coils were also required whenever zero field (± 0.1 G) was needed to compensate for the residual magnetism of the electromagnet and in view of the fact that the main magnet power supply was not capable of delivering very low currents. The current to the coils was supplied by a Harrison Model 814A power supply.

The d.c. current-regulated power supplies for M_1 and M_2 have been previously described (Colclough 1963). They have a maximal output of 8.5 kW (short term) and 3.2 kW (continuous) and are stable to one part in 10^4. The helipot control on each unit was fitted with a slow, three-speed synchronous motor drive which permitted smooth scanning of the magnetic field. When required, the drive could be disengaged by means of an overriding clutch to permit manual adjustment of the helipot setting. An alternative SCR Model 120-40 power supply was used in conjunction with M_1, to produce magnetic fields in the range 0-0.5 kG.

The magnetic fields were measured by an R.F.L. Model 1890 gaussmeter which employed a hermetically sealed indium arsenide Hall probe. The gaussmeter was calibrated for zero and for the one kG range by the use of a zero-gauss

chamber and reference magnet, and the probe was then secured
to the pole face of the magnet where its position was adjusted
for maximal field strength. Magnetic fields from 0.1 G to
20 kG could be measured with an accuracy of three percent.

The water lines supplying the electromagnet were
fitted with water filters and flow meters. The latter, con-
nected to the power supply, served as a protection against
inadequate flow rate of cooling water to the magnets.

(c) The Fluorescence Cells

The fluorescence cell in which resonance fluores-
cence was excited with unpolarized light is shown in Figure
12. The arrangement of three mutually perpendicular windows
forming a rectangular corner, permitted excitation by a light
beam perpendicular to the field and observation of fluorescent
light emitted in a direction parallel to the field. The
outside of the cell, especially near the region of fluores-
cence, was coated with Aquadag. This reduced the effect of
scattered light, limited observation to the region immediately
adjacent to the corner between the windows, and resulted in
minimal reabsorption of both exciting and fluorescent light.
The cell had a short side-arm which contained approximately
1.5 g of cesium metal and was connected to the vacuum and
gas filling system by a 2 mm capillary. The cell was mounted
in an oven, between the pole pieces of the magnet M_2. The
oven consisted of two parts: an outer rectangular panelyte
box and an inner box of 1 mm-thick copper plate with provision

Figure 12. A sketch of the fluorescence cell used for studies of fluorescence emitted at right-angles to the direction of excitation.
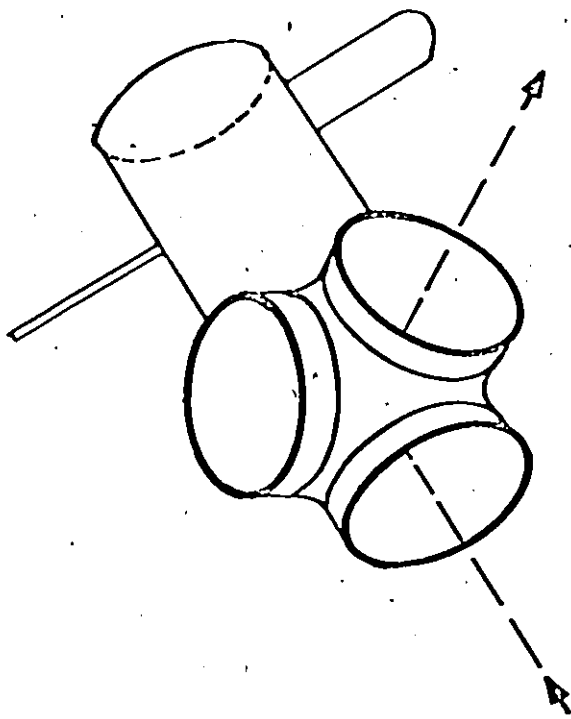
for access to the various cell windows and to the side-arm

assembly. Non-inductively wound heating elements, insulated

by asbestos paper, were placed between the inner and outer walls

of the oven. The elements were made of #28 thermal heating wire

wound on asbestos paper, and had a total parallel resistance

of 4.8Ω. A side-oven, consisting of a machined brass cylinder

attached to the bottom of the main oven, was closely fitted

to the side-arm with good thermal contact provided by sheets

of thin copper foil. Temperature stability of the side-oven,

within $\pm0.3^\circ C$, was maintained by a Jena Ultrathermostat which

circulated warm water through a 1/4 in. coil of copper tubing

snugly fitted to the side oven and thermally insulated from

the outside by a layer of asbestos tape. Temperatures were

measured by thermocouples which were attached to the cell

near the entrance and observation windows and near the side-

arm, and which were connected to a Leeds and Northrup Model

8686 potentiemeter. A thermistor attached to the base of

the cell was connected to the temperature controller which

provided temperature stability in the main oven to within $\pm1^\circ C$.

The fluorescence cell in which resonance fluores-

cence was excited with polarized light directed parallel to

the field M_2, is depicted in Figure 13. The cell, constructed

of pyrex, is of a single window, "Wood's-horn design". The

sharply angled rear portion of the cell minimized reflections

and limited light paths in the vapour. In addition, to reduce

surface reflections, the window of the cell was canted through

an angle of approximately 5° about an axis perpendicular to

Figure 13.   A sketch of the fluorescence cell used for studies of fluorescence emitted anti-parallel to the direction of excitation.
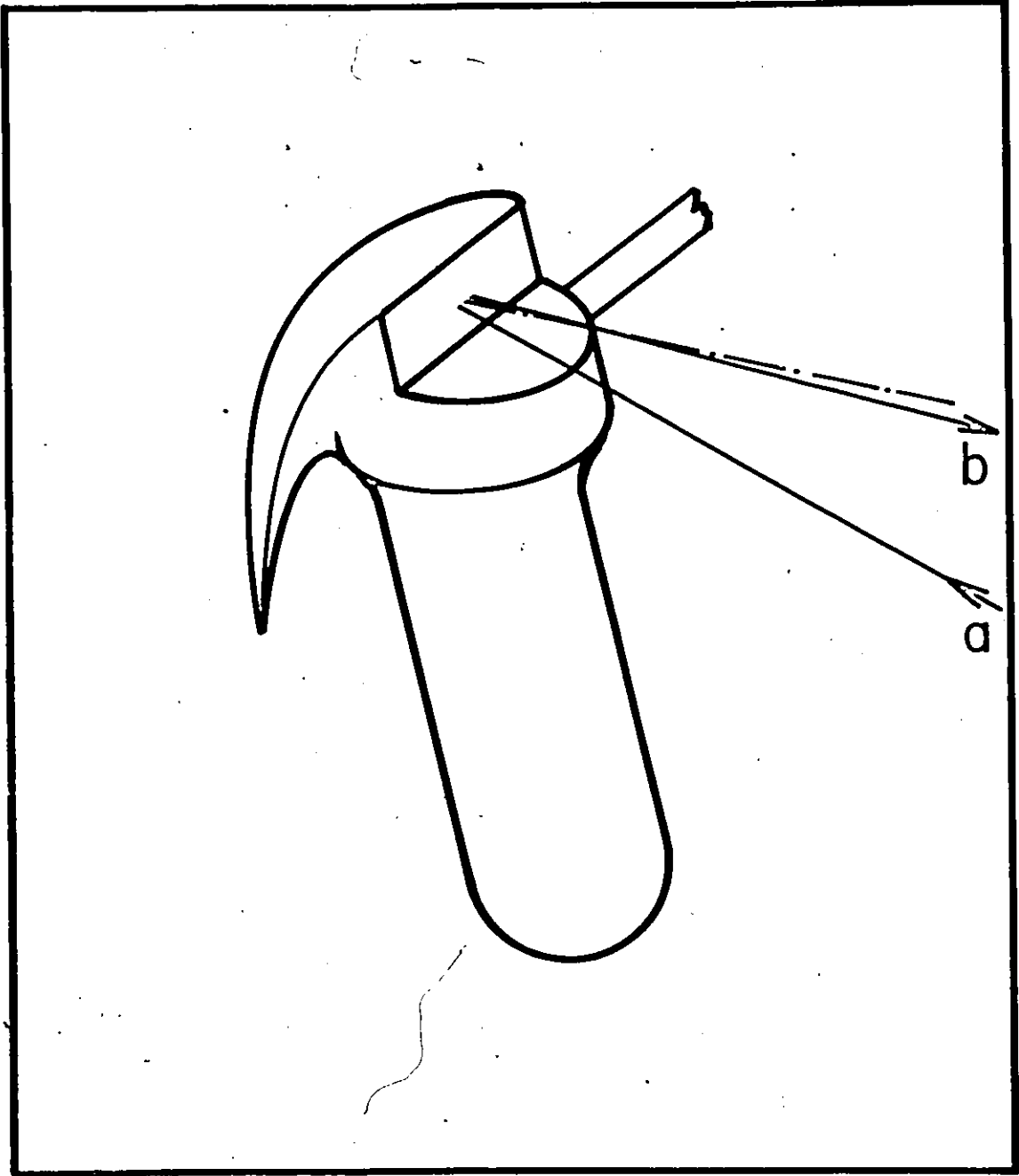
the plane of the exciting and fluorescent light beams. The
cell was mounted in an oven, between the pole pieces of
the magnet M_2. The oven consisted of two parts. The princi-
pal portion was a rectangular panelyte enclosure in which
heating was provided by warm air circulating about the main
body of the cell and supplied through a heavy-paper tube
from a heater which consisted of an electric heating element
and fan mounted outside of the magnetic field region. Main
oven temperatures were maintained at $43^{\circ}C$ with stability
better than $\pm 1^{\circ}C$. The side-oven assembly was identical to
that described above. Temperatures were measured with
thermocouples attached to the cell at the top and sides of
the window and to the side-arm.

(d) The Optical System

The principal features of the optical system em-
ployed in the fluorescence experiments, in which unpolarized
light was used for excitation, are shown in Figure 10. The
condensing lenses in the exciting light beam were chosen so
as to provide maximal light flux at the fluorescence cell
while, at the same time, allowing the lamp to be kept at a
distance of about 1 m from the magnet, to reduce the effect
of the magnetic field on its performance. The Spectrolab
interference filters transmitted approximately 85 per cent
of the 8943-$\overset{\circ}{A}$ component. The lenses in the fluorescent light
beam, one of which was mounted in the pole-piece aperture,
were chosen to gather the maximal amount of the fluorescent
light and focus it at the photocathode of the phototube. The

circular analyzer consisted of a quartz $\lambda/4$ plate 25 mm in diameter, supplied by the Industrial Optics Co. of Newark, New Jersey and a Glan-Thompson prism with a transmission of 45% for unpolarized light and an extinction ratio greater than 10^4:1. This combination produced circularly polarized light to within 1%.

The experiments using polarized exciting light required modifications of this system, as may be seen in Figure 11. The exciting light from the spectral lamp, before reaching the fluorescence cell, passed through a defining aperture, prism, interference filter and polarizer, and was reflected in a front-surface aluminized mirror. The polarizer was either circular, consisting of an HR polaroid and a $\lambda/4$ plate, or linear (HR polaroid). The 4 x 2.5 cm mirror, which could be rotated about the vertical axis and translated in a horizontal plane, produced maximal incident light flux at the cell, without obstructing the fluorescent light beam from the cell, which was passed through a 9 cm f.l. lens mounted in the pole-piece aperture, a circular analyzer and an 8 cm f.l. lens mounted before the phototube. The circular analyzer consisted of two mica $\lambda/4$ plates with their "fast axes" set at 90° to each other and an HR polaroid with the transmission axis bisecting the angle between the "fast axes" of the $\lambda/4$ plates.

The $\lambda/4$ plates were mounted in an automated carriage which positioned them alternately in the fluorescent light beam. During the experiment involving linearly polarized light, two polaroids with crossed transmission axes were mounted in the carriage replacing the $\lambda/4$ plates..

The light output of the spectral lamp decreased when the field M_1 was increased from 0.4 kG to 8 kG. Thus in experiments with the lamp in a field of 8 kG, a lock-in system was used to register the fluorescent light. To this purpose, the fluorescent light was modulated with a special mechanical light chopper (PAR Model 125). The eight slots in the chopping wheel held pieces of HR polaroid whose transmission axes were alternatively inclined at 90° to each other. The resulting signal from the photomultiplier was applied to the input of a PAR Model H.R.8 lock-in amplifier to which a reference signal was provided directly from the chopper. The frequency of the chopper was set at 333 Hz and the reference frequency at 167 Hz. The output signals of the lock-in amplifier at frequencies of 167 Hz and 333 Hz were proportional to $I_{\sigma^+} - I_{\sigma^-}$ and $I_{\sigma^+} + I_{\sigma^-}$, respectively (see Appendix A). The degree of polarization could thus be obtained in a straightforward manner.

The $\lambda/4$ plates, used in the circular polarizers and analyzers, produced polarized light circular to within 3% (based on ellipticity). The principal transmittances K_1 and K_2 of HR are, respectively, 77% and less than 1% at 8943-Å, and 68% and less than 1% at 8521-Å (as specified by the manufacturers).

(e) The Detection System

The fluorescent radiation was monitored by an FW118, 16 dynode I.T.T. photomultiplier tube with an S1

(Ag-O-Cs) photocathode which has a peak sensitivity in the 8000 $\overset{o}{A}$ region. High voltage to the phototube was supplied from a Fluke model 412B power supply operated at 1500-1700 V, through a resistive divider chain providing 85-96 V per stage. The phototube was shielded against external magnetic fields, and was housed in a liquid nitrogen-cooled cryostat with the result that it had background noise of less than 10^{-13}A. In most of the experiments its output was amplified by a Keithley 417 high-speed picoammeter equipped with variable damping and high suppression current adjustment. The latter feature permitted current suppression at the input of up to 1000 times full scale deflection, allowing large-scale display of 0.1 per cent variation in the signal. The amplified signal was applied to the Y axis of a Hewlett-Packard Model 20 X-Y plotter, the X axis of which was connected to the output of the gaussmeter.

(f) The Vacuum and Gas-Filling System

The vacuum in the system which was constructed of pyrex glass, was generated by an Edwards Model EO2 water-cooled oil diffusion pump filled with No. 704 silicone pumping fluid and backed by an Edwards Model ES35 single stage rotary pump. With a liquid nitrogen trap, vacua of the order of 5×10^{-8} torr were attained. Damage due to water and/or power failure was prevented by using a line relay switch in addition to an Edwards thermal switch on the diffusion pump which was also equipped with an Edwards electromagnetic backing valve.

A C.V.C. Model GIC-110 ionization gauge served to measure the vacuum, and an Autovac Model 3294-B gauge was used for approximate measurements of gas pressure. Accurate pressure readings were obtained with a C.V.C. Model GM-100A trapped McLeod gauge. When not in use, the latter was isolated from the main vacuum system to minimize the possibility of mercury contamination.

The gas-filling assembly included several pyrex 1-litre flasks containing samples of the various noble gases, as well as two flasks containing a few grams each of potassium or cesium metal. The latter flasks, when heated, served as noble gas getters and were connected to the vacuum system by means of a parallel arrangement of coarse- and capillary-bore stop cocks. This feature permitted rapid filling and evacuation of the flasks as well as the metered admission of gettered gas to the fluorescence cell.

During the investigation, the vacuum system was improved by the substitution of 705 silicone pumping fluid and the increase of the diameter of the main manifold from $\frac{1}{2}$ in. to 1 in. Dynamic vacua in the modified system were typically better than 5×10^{-9} torr, and static vacua better than 10^{-7} torr could be maintained for periods in excess of 24 hr.

The entire system was fastened to a rigid aluminum frame mounted on casters, which straddled the pedestal mount of the magnet M_2 and allowed easy and precise positioning of the fluorescence cell between the pole pieces.

2. Experimental Procedure

(a) Preparation of Fluorescence cells and buffer gases

Identical cleaning and filling procedures were followed with the two fluorescence cells which have been described in Section IV(c). Before use, each cell was cleaned with dichromate cleaning solution and rinsed thoroughly with distilled water. It was then dried, attached to the vacuum system and outgassed for several hours at a temperature of about 150°C at a vacuum of 10^{-7} torr. An ampoule containing cesium of 99.95% purity (supplied by the A.D. McKay Co.) was broken under vacuum and about 1 g of the metal was distilled into the cell and side-arm. Distillation into the side-arm was completed (under vacuum) by installing the cell in its oven, in which a temperature of 150°C was maintained for several hours, while the side-arm temperature was kept at 20°C by circulating cooling water through the side-oven coil. Thermistors and thermocouples were fastened in position using rubber cement and the cell was properly enclosed in the oven.

The 3-window cell, mounted in its oven, was positioned between the pole pieces of magnet M_2 and aligned, using a light beam which passed through both pole-piece apertures, so that the corner between the windows was clearly illuminated when viewed through one of the apertures. The position of the one-window cell was adjusted by using a

cathetometer to centre the upper portion of the window of
the cell with respect to the pole-piece aperture and to
locate the cell in the centre of the magnetic field region.
After completion of the optical alignment, the fluorescence
cell was reconnected to the vacuum system by means of a
4 mm (i.d.) tube.

Several days before an experimental run, noble gas
was introduced into one of the evacuated alkali metal-coated
getter flasks. Getter temperatures in excess of 400°C were
maintained for not less than one week, using electric heating
tapes. Several hours before the gettered sample was to be
used, the getter was chilled by immersion in a dewar flask
containing either liquid nitrogen or, in the case of krypton
and xenon, a mixture of dry ice and methanol.

(b) Fluorescence Experiments with Unpolarized
8943 $\overset{o}{A}$ Exciting Light

The optical elements in the exciting light beam
were positioned and aligned with respect to the fluorescence
cell and to the direction of the magnetic field, with the aid
of a cathetometer. The rf oscillator was set for maximal
output (150-200 mA, 325-375 V) by adjusting the input voltage
and current, and modifying the configuration of the tank coil.
After the bulb had been glowing for approximately 30 min.,
the temperature of the side-arm was adjusted (a temperature
of 70°C was eventually selected for optimal conditions).
An unresolved beam of Cs resonance radiation was focussed in

the cell, and the resulting fluorescence was detected with the photomultiplier, whose signal was registered on the linear scale of the picoammeter. The output of the latter was applied to the Y axis of the X-Y plotter and the signal fluctuations were used to verify the linearity of the plotter, whose X axis was calibrated in gauss using the output of the gaussmeter.

Interference filters were placed in the collimated portions of the beam. They and all the other elements of the optical system were adjusted in turn, until a maximal signal and minimal background were indicated by the X-Y recorder. The Glan-Thompson prism and $\lambda/4$ plate were then inserted in the fluorescent light beam and the magnetic field was scanned to produce a trace similar to that shown in Figure 2(b). The circular polarization of the fluorescent light was maximized by adjusting the polarizer and $\lambda/4$ plate.

A non-fluorescent (background) contribution to the signal was found to be approximately 1%, by freezing the side-arm to -60°C.

The onset of radiation trapping was determined by monitoring the fluorescent intensity at zero M_2 field, in relation to Cs vapour pressure, and was found to take place at approximately 32°C which corresponded to a Cs vapour pressure of 2.6×10^{-6} torr. Because the measurements were to be carried out at a relatively high magnetic field value and because there was ample fluorescent intensity available, the operating temperature was lowered to 28°C and the Cs

vapour pressure to 1.7×10^{-6} torr, thus ensuring the absence
of effects due to radiation imprisonment. Lamp stability
was verified by monitoring the fluorescent intensity at
zero M_2 field over periods of several hours.

The fluorescent intensity peaks observed in the
vicinity of 9.8 kG were scrutinized with respect to intensity,
resolution and polarization. If required, the lamp temper-
ature was adjusted to obtain peaks of maximal intensity and
minimal width, and free of self reversal.

The main peak heights in the recorder trace shown
in Figure 2(b) were used, in conjunction with Eq. (II-1), to
determine the degree of polarization in pure cesium vapour.
Gettered noble gas was then introduced into the fluorescence
cell. After equilibrium was established, the scanning pro-
cedure was repeated for a range of noble gas pressures
extending from about 0.2 torr to 10 torr.

A typical intensity scan required a time of approx-
imately 8 min., during which fluctuations in lamp intensity
were negligible.

(c) Fluorescence Experiments with Polarized
Exciting Light

Because of the geometry employed, a large propor-
tion of the light reaching the photomultiplier was due to
reflection of the exciting light from the window of the cell.
To minimize this contribution, the window was tilted at ap-
proximately 5° to the direction of the magnetic field, thus

increasing the proportion of fluorescent light in the total
signal, to 15-20%, which was achieved upon careful adjust-
ment of the lens system, lamp prism and cell mirror.
As the temperature of the side-arm of the cell was reduced
to less than $-30^{\circ}C$, the fluorescent intensity at zero M_2
field decreased to a point indistinguishable from the back-
ground and from the level registered at $M_2=10$ kG, at which
the signal was insensitive (within 1 per cent) to variations in
Cs vapour pressure. With $M_1=0.4$ kG and $M_2=10$ kG, there is
virtually no fluorescent emission because of the Zeeman
splitting of the absorption line. It was therefore found
convenient to take the signal registered at $M_2=10$ kG, as the
zero reference level for the fluorescent intensity.

As interference filters and circular analyzers
were inserted in the light paths, the magnetic field (M_2)
scans produced traces such as are shown in Figures 3 and 5
representing circular polarization of the $^2P_{\frac{1}{2}}$ and $^2P_{3/2}$
states, respectively. The degree of polarization P at
points along the profiles was determined in accordance with
Eq.(II-1). The value of P is particularly important at
zero M_2 field and at the highest field-values at which mean-
ingful measurements of intensity levels could be obtained.

Imprisonment of resonance radiation is more pro-
nounced at zero field than at kG fields, because of decreased
reabsorption resulting from Zeeman splitting. In the presence
of radiation imprisonment, P_0 decreases with increasing

vapour pressure and the variation of fluorescent intensity with vapour pressure becomes non-linear (Chapman 1965). The values of P_O for $M_2 = 0.0$ kG and $M_2 > 5$ kG were determined and compared to the theoretically calculated values. The presence of radiation imprisonment was thus detected. For $M_2 = 0.0$ kG, the theoretical values of P_O for the $^2P_{\frac{1}{2}}$ and $^2P_{3/2}$ states are 0.344 and 0.479, respectively. At high magnetic fields, $P_O = 1.0$ for both states. In the absence of radiation imprisonment, the ratios of P_O at 0.0 kG and high magnetic fields should therefore approach 0.344 and 0.479 respectively. Actual P_O values determined in various experiments will be discussed in a subsequent section.

By monitoring the fluorescent intensity and P_O in relation to the Cs vapour pressure, the following operating values for the vapour pressure were determined, at which radiation trapping was absent. For the $^2P_{\frac{1}{2}}$ state ($8943-\text{\AA}$) with $M_1 = 0.4$ kG, 1.7×10^{-6} torr; with $M_1 = 8$ kG, 2.6×10^{-6} torr. For the $^2P_{3/2}$ state ($8521-\text{\AA}$), 7.7×10^{-7} torr.

In the investigation of $^2P_{\frac{1}{2}}$ disorientation, the experiments at low and high magnetic fields were carried out under somewhat different conditions and in slightly different ways. In the range $M_2 = 0 - 6.3$ kG, M_1 was held at 0.4 kG and the photomultiplier tube was used in the d.c. mode. The $M_1 = 0.4$ kG field produced a broad exciting line free of self reversal, permitting more efficient excitation than with $M_1 = 0.0$ kG. When measurements were carried out at $M_2 > 6.3$ kG,

M_1 was held at 8 kG, increasing the efficiency of excitation, and the fluorescent signal was detected with the aid of a lock-in amplifier. The fluorescence cell was evacuated and lamp stability was verified. Intensity profiles σ^+ and σ^- were scanned several times and polarization values were determined at intervals of approximately 0.33 kG ranging from 0.0 kG to 5.7 kG for different values of He pressure not exceeding 10 torr. A similar procedure was followed for $M_1 = 8$ kG except that measurements were restricted to values of M_2 in the vicinity of 8 kG.

In the case of the $^2P_{3/2}$ state, $M_1 = 0.4$ kG and measurements of depolarization induced in collisions with He, Ne, Ar, and Xe atoms at low pressures were carried out.

Because of the proximity of the magnet M_2 to the phototube, the photomultiplier signal, on at least two occasions, exhibited anomalous behavior directly attributable to magnetic field effects. Such effects, due to deterioration of the netic - conetic phototube shield, manifestly altered the background reference level. Consequently, at the beginning of each experimental run, a record was made of the background level which was invariant with respect to the strength of the field M_2. When any deviation became apparent, the photomultiplier was tested for sensitivity to magnetic field by slowly varying the position of a permanent magnet in its vicinity. Any failure of the magnetic shielding would manifest itself as a variation in the signal,

similar to that produced by scanning M_2. The photomultiplier
assembly would then be removed from the cryostat housing
and the magnetic shield replaced. The useful lifetime of
such shields could be as short as 6 months.

V. DISCUSSION OF RESULTS

1. Disorientation of $6^2P_\frac{1}{2}$ Cs Atoms by Collisions with
   Noble Gases

Figure 2(b) shows the recorder traces obtained in
a magnetic field scan of the relative fluorescent intensities
I_{σ^+} and I_{σ^-} observed in a direction parallel to the field
M_2 in the vicinity of 9.8 kG, and using unpolarized exciting
light incident in a direction perpendicular to M_2. Repeated
scans at various noble gas pressures in the range 0 - 10 torr
yielded several values of I_{σ^+} and I_{σ^-} which were substituted
in Equation (II-1), yielding the degrees of polarization P
which are plotted in Figure 14 against the gas pressures. The
values of P and the corresponding pressures were fitted by the
method of least squares to Equations (III-3) and (III-4) which
yielded the disorientation cross sections σ_1 shown in Table
3. Not less than 25 separate measurements were involved in
the determination of each cross section and each set of data
was acquired in at least two experimental runs to ensure re-
producibility. That the factors P_0 differ from unity is due
principally to the finite angle subtended by the photomulti-
plier at the fluorescence cell, and to inexact collimation
of the fluorescent light beam.

The peaks at 9.8 kG shown in Figure 2(b) were fitted
to a Gaussian profile in order to establish the degree of
resolution of these peaks from those in their immediate vici-
nity, and the effect of resolution on the values of the

Figure 14. Variation of the degree of polarization of the 8943-$\overset{o}{A}$ resonance fluorescence at 9.8 kG with noble gas pressure. Unpolarized light was used for excitation.

Xe, Kr, PRESSURE (Torr)

Xe

Kr

Ne

P

Ar

He

Ne, Ar, He, PRESSURE (Torr)
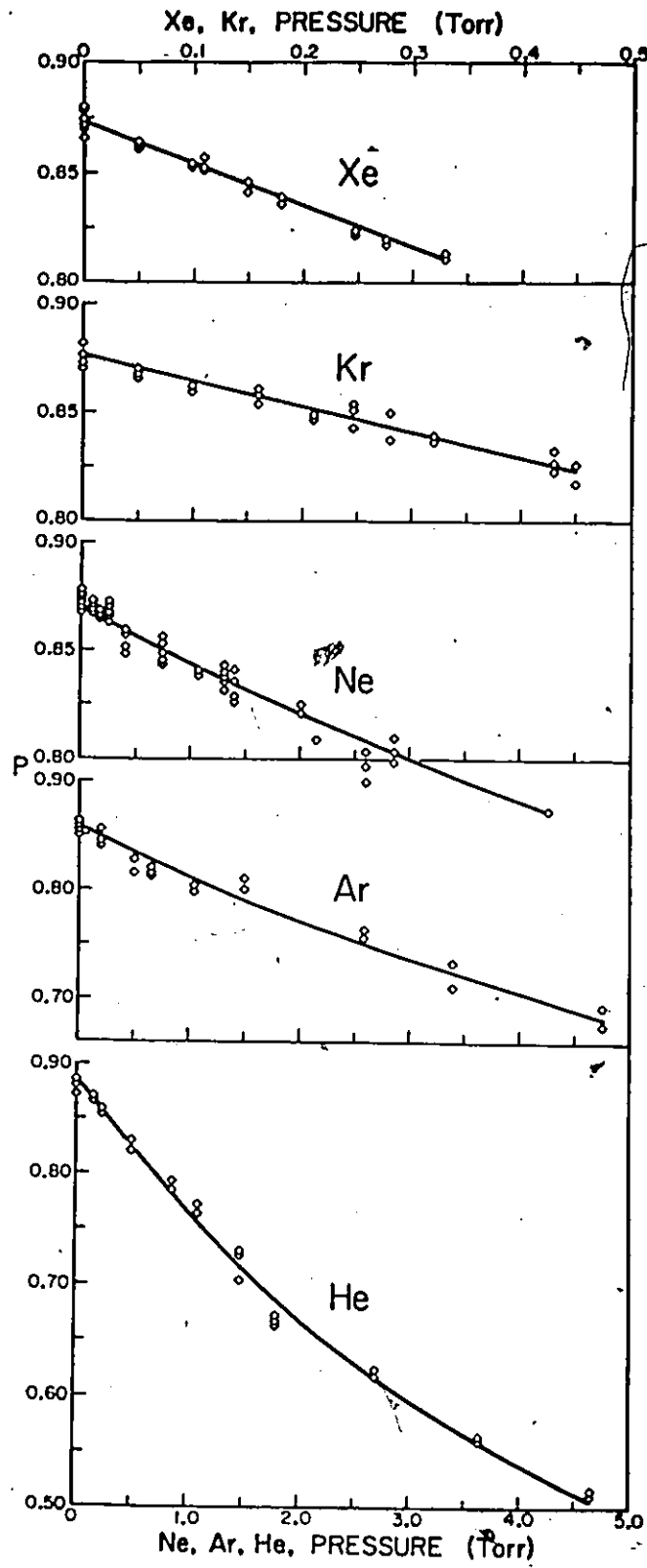
TABLE 3

Cross sections for disorientation of the $6^2P_{1/2}$ Cs atoms. All values are given in Å².

Collision Partners	This Investigation		Zero Field			Theoretical	
	9.8 kG	0.0 - 8.0 kG	Bulos and Happer (1971)	Franz and Sooriamoor- thi (1974)	Niewitecka and Krause (1976)	Gordeev et al. (1969)	Roueff and Suzor (1974)
Cs - He	11.8 ± 1.8	6.0 ± 0.9 - 11.1 ± 1.6	6.1	12.5 ± 4.0	4.9 ± 0.7	9.0	10.8
Cs - Ne	4.7 ± 0.7		2.3	6.9 ± 2.0	2.1 ± 0.3	9.1	
Cs - Ar	10.7 ± 1.6		5.0		5.6 ± 0.8	9.3	
Cs - Kr	37.9 ± 5.7				5.8 ± 0.9	9.6	
Cs - Xe	71.7 ± 10.8				6.3 ± 0.9	9.7	

cross sections. The cross sections determined in this way did not differ significantly from those obtained from direct peak intensity measurements of the $I_{\sigma+}$ and $I_{\sigma-}$ components.

The circular depolarization of the 8943-Å resonance fluorescence, induced by He collisions, was also studied over a range of fields from zero to 8.0 kG, to investigate the effect of the magnetic field on the disorientation cross sections. The excitation took place with circularly polarized light directed along the magnetic field axis, and the partly depolarized fluorescence was observed in the backward direction. The variation of the degree of polarization with He pressure was determined from magnetic field scans similar to those shown in Figures 3 and 4. Figure 15 shows several plots of the degree of polarization against He pressure, each corresponding to a particular value of the magnetic field. The density of the points, their scatter and indicated deviations, are typical of all the data which were taken off the recorder traces at 0.3 kG intervals.

The depolarization data obtained in zero field was analyzed using Equations (III-3) and (III-6). Equation (III-6) takes into account the effects of nuclear spin on the relaxation process, whereas Equation (III-3) does not. It was found that the cross sections obtained by either treatment are not significantly different, as might have been expected. (See Section III-1.) Equation (III-3) was used exclusively for the analysis of all results obtained at kilogauss fields at

Figure 15.   Variation of the degree of polarization
of the 8943-Å resonance fluorescence with He pressure at
various magnetic fields as indicated in kilogauss. σ^+
polarized 8943-Å light was used for excitation.
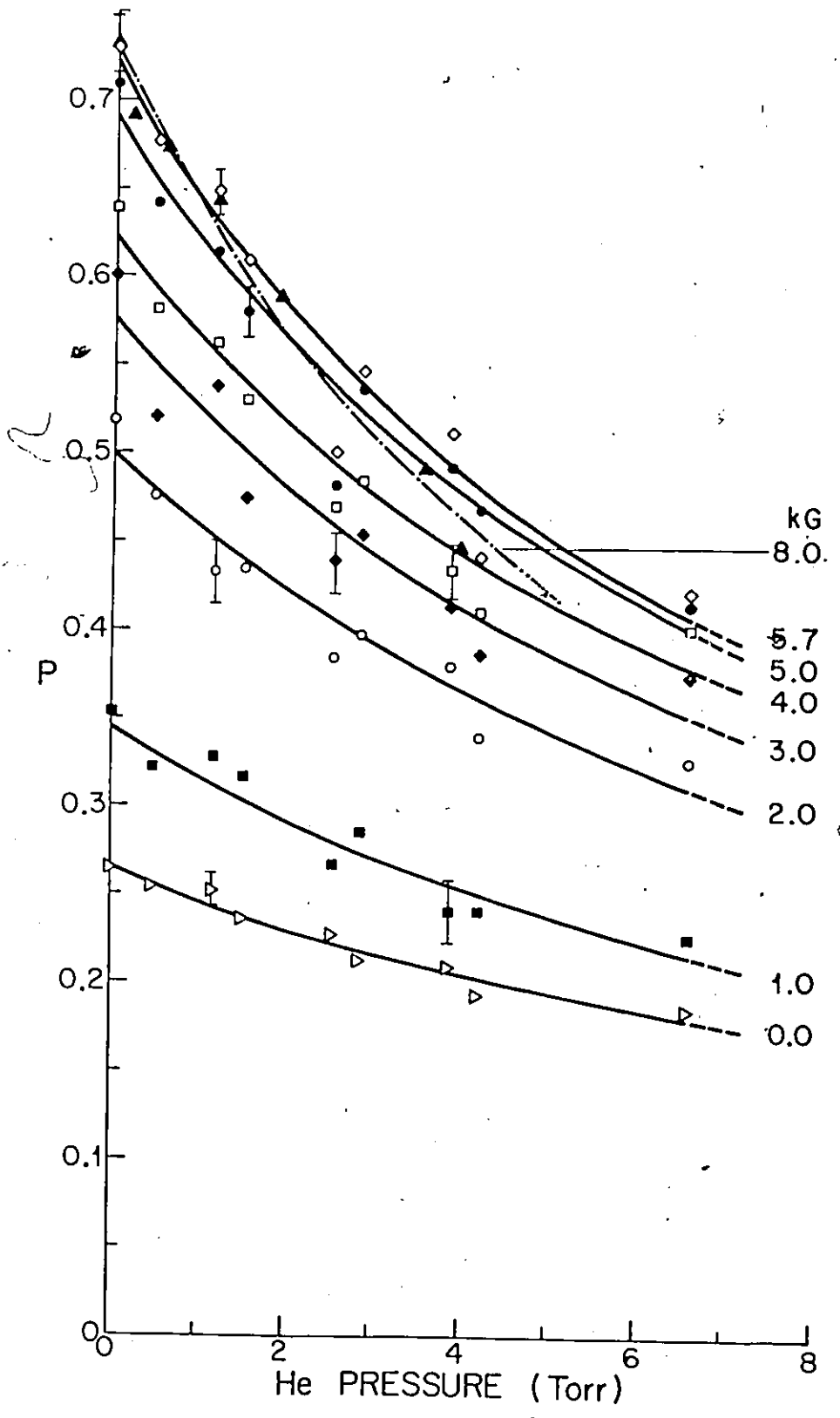
which the nuclear spin is completely decoupled and has no effect on the experimental observations. The cross sections yielded by the various experiments are summarized in Table 3, which also includes experimental and theoretical values reported by other authors.

As may be seen from Figure 16, which shows a plot of disorientation cross section against magnetic field, the cross sections exhibit a pronounced dependence on magnetic field strength. The value obtained at zero field agrees with that quoted by Bulos and Happer (1971) who corrected Gallagher's (1967) Hanle-effect data for the effect of nuclear spin, and with the most recent results obtained by Niewitecka and Krause (1976), but is significantly lower than the values calculated by Gordeev et al. (1969) and by Roueff and Suzor (1974). Unfortunately, no explanation can be offered for the discrepancy with the low-field cross section determined by Franz and Sooriamoorthi (1974), which is close to the values measured at high magnetic fields but substantially exceeds other low-field or zero-field cross sections.

It has been suggested that the magnetic field-dependence of the disorientation cross sections might be caused by magnetic field-induced $^2P_{1/2}$ - $^2P_{3/2}$ mixing, which contributes to the depolarization mechanism (Baylis 1971). The observed variation with magnetic field strength, as shown in Figure 16, may be represented by the relation

(V-1) $\sigma_1(B) = \sigma_1(0) + K\ B^{1.8}$

Figure 16.   Variation of the $^2P_{1/2}$ disorientation cross section with magnetic field.
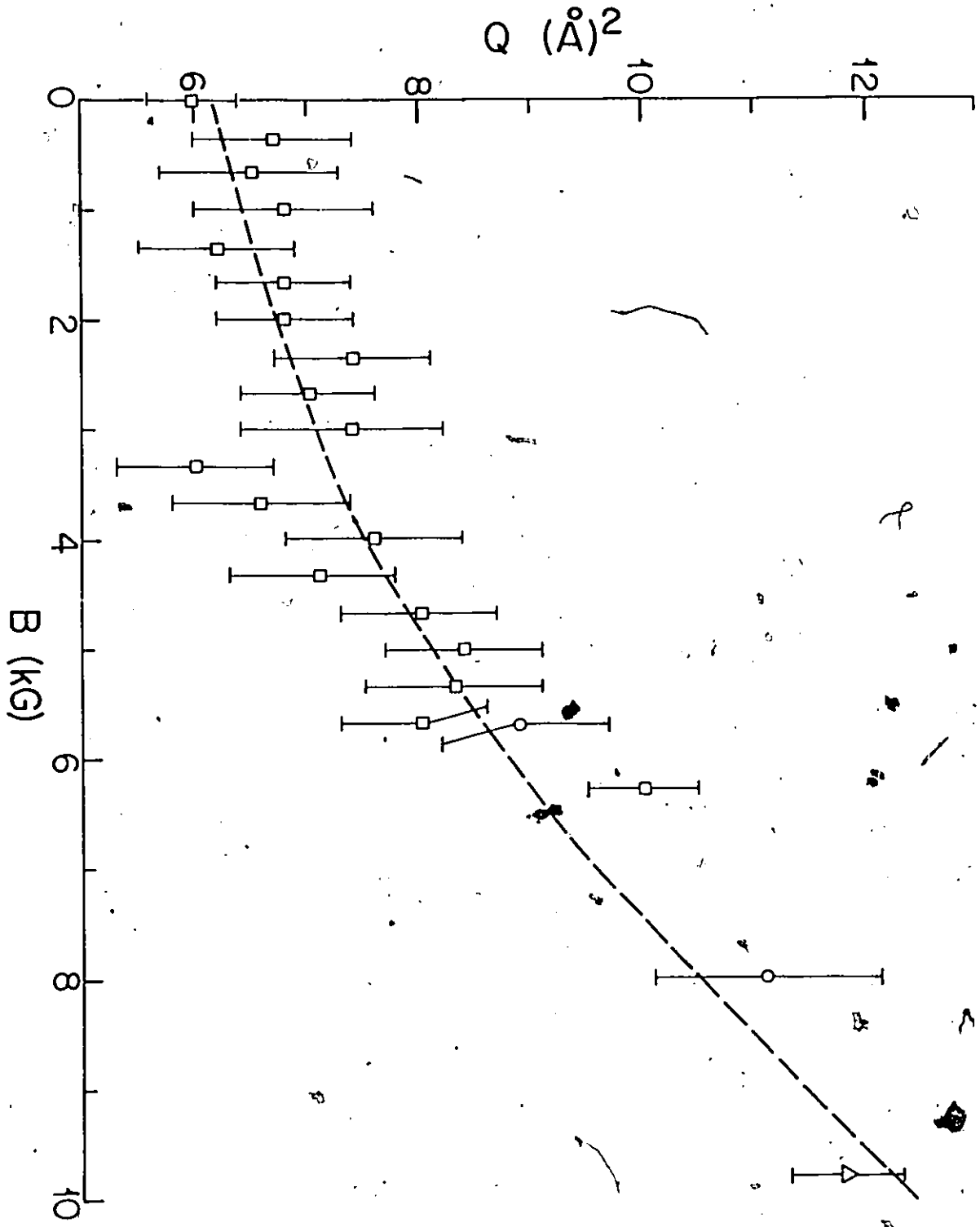
where $\sigma_1(B)$ and $\sigma_1(0)$ are the cross sections at field B
and at zero field, respectively, and K is a constant. This
behavior of the cross sections is in good agreement with
theoretical predictions (see Appendix B).

There is, unfortunately, almost no other informa-
tion available on the magnetic field-dependence of disorienta-
tion cross sections. Berdowski and Krause (1968) used Zeeman
scanning to determine the disorientation cross sections for
the $4^2P_{\frac{1}{2}}$ state in potassium at 5 kG which are presented in
Table 4 together with the most recent values obtained at
zero magnetic field (Niewitecka and Krause 1975). It appears
that, in the case of potassium, the high-field cross sections
are also significantly larger than the zero-field values.

TABLE 4

Cross sections for disorientation of $4^2P_{1/2}$

K atoms by collisions with noble gases

Collision Partners	Collision cross sections ($Å^2$)	
	At zero field Niewitecka and Krause (1975)	At 5 kG Berdowski and Krause (1968)
K - He	24 ± 4	46
K - Ne	21 ± 3	39
K - Ar	37 ± 5	52
K - Kr	51 ± 7	79
K - Xe	79 ± 9	108

2.   Depolarization of $6^2P_{3/2}$ Cs Atoms Induced in Collisions With Noble Gas Atoms

The depolarization of $6^2P_{3/2}$ Cs atoms induced in collisions with noble gases, was investigated using the apparatus shown in Figure 11. Circularly or linearly polarized radiation emitted from the spectral lamp located in the field M_1=0.4 kG was made incident on the fluorescing vapor-gas mixture, in a direction parallel to the field M_2 and was observed in the anti-parallel direction.

The relative intensities of circularly polarized fluorescent components $I_{\sigma+}$, $I_{\sigma-}$ and linearly polarized components $I_{\pi+}$ and $I_{\pi-}$ were recorded in repeated scans of M_2, to determine the appropriate degrees of polarization P_σ and P_π at various noble gas pressures. P_σ was found by substitution in Equation (II-1) and P_π is given by

$$(V-2) \quad P_\pi = \frac{I_{\pi+} - I_{\pi-}}{I_{\pi+} + I_{\pi-}}$$

where π^+ and π^- indicate two mutually perpendicular components of linear polarization with π^+ parallel to the lamp-cell axis.

P_σ or P_π, used in conjunction with Equation (III-3) or Equations (III-21) and (III-22), permit the calculation from experimental data of the cross sections for circular and linear depolarization induced by collision with noble gas atoms.

Figure 5 shows the $I_{\sigma+}$ and $I_{\sigma-}$ fluorescent intensity

profiles obtained in a magnetic field scan, with σ^+ light used for excitation. The two intensity maxima near zero field and 6 kG result from various coincidences between the Zeeman components in emission from the lamp located in a 0.4 kG field, and in absorption by the cesium vapor in the cell. The peak near zero field arises from a maximal overlap between the spectral components in emission and absorption, corresponding to the $\Delta m = +1$ transitions between the $^2S_{1/2}$ and $^2P_{3/2}$ states. The broad peak centred at 6 kG is due to coincidences between the Zeeman components in the exciting light and transitions to the various m_I sublevels of the $m_J = +3/2$ Zeeman substate in the absorbing cesium atoms; because of broad-line excitation, transitions involving individual m_I sublevels are not resolvable. The identification of the maxima in Figure 5 was made on the basis of approximate Breit-Rabi calculations of Zeeman splittings (Breit and Rabi 1931), followed by a rough modelling of the intensity profile.

Figure 6 represents $I_{\pi+}$ and $I_{\pi-}$ fluorescent intensity profiles obtained in a similar magnetic field scan, with π^+ light used for excitation. The fluorescence arises from $\Delta m = 0$ transitions between the $^2S_{1/2}$ and $^2P_{3/2}$ states, with the axis of quantization parallel to the $\vec{E}$ vector of the exciting beam and perpendicular to the magnetic field axis. Consequently, one should expect a noticeable difference between $I_{\pi+}$ and $I_{\pi-}$ only at low fields, and rapid depolarization at higher fields, resulting from the increasing

rate of precession of the atomic dipole about the magnetic field axis.

The appropriate P_σ and P_π were extracted from repeated magnetic field scans at noble gas pressures ranging from 0 to 3 torr. Plots against noble gas pressures are shown in Figures 17 - 22. At least 25 separate scans were carried out in several sequences, to ensure reproducibility. The data corresponding to low magnetic fields were fitted to Equation (III-3) and the P_σ values obtained at kilogauss fields were fitted to Equation (III-21). The least-squares analyses yielded the relevant depolarization cross sections.

The interpretation of the high-field measurements is relatively simple because the nuclear spin is completely decoupled, with the result that $Q(circ.) \equiv \sigma_1$, and $Q(lin.) \equiv \sigma_2$. Equation (III-21) involves the two relaxation rates γ_1 and γ_2, and the least-squares analysis yields σ_1 and the ratio σ_2/σ_1, both of which can be obtained from the experimental results without assuming any particular model for the interaction. An alternative approach to the treatment of the data would involve the assumption of a particular value for the ratio γ_2/γ_1, derived from one of the models considered appropriate for the interaction (e.g. the van der Waals' model). Although this procedure was not adopted ultimately, a sensitivity test suggested that, as γ_2/γ_1 was assigned various values between 1.0 and 2.0 (corresponding to the various models), the resulting value of σ_1 varied

Figure 17.   Variation of the degree of circular

polarization of the 8521-$\overset{o}{\text{A}}$ resonance fluorescence with

noble gas pressure at zero field. σ^+ polarized 8521-$\overset{o}{\text{A}}$

light was used for excitation.

Figure 18.   Variation of the degree of circular

polarization of the 8521-$\overset{o}{A}$ resonance fluorescence with

noble gas pressure at 0.6 kG.

Figure 19. Variation of the degrees of circular polarization of the 8521-Å resonance fluorescence with noble gas pressure at 3.8 kG.

Figure 20.   Variation of the degree of circular polarization of the 8521-Å resonance fluorescence with noble gas pressure at 5.3 kG.
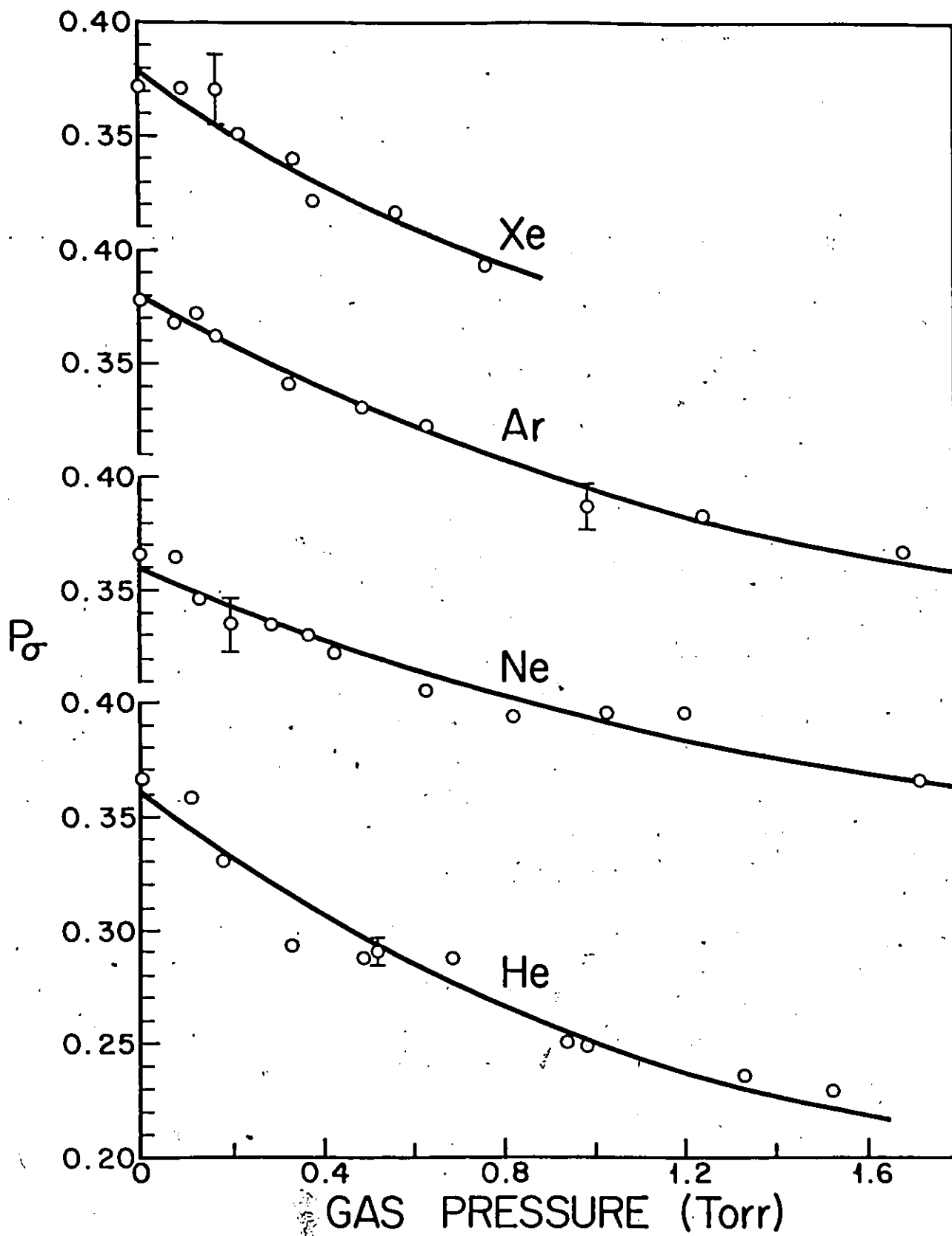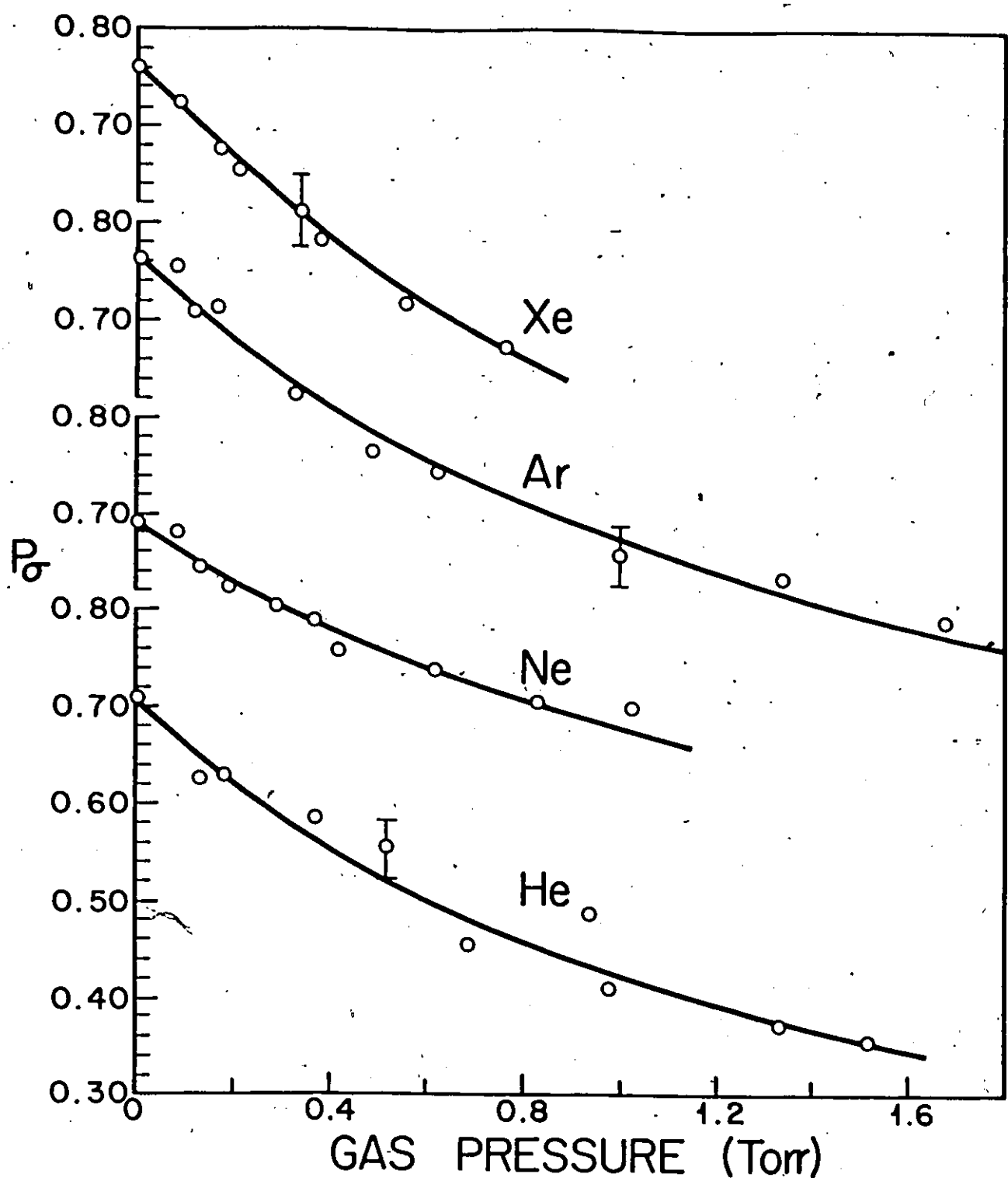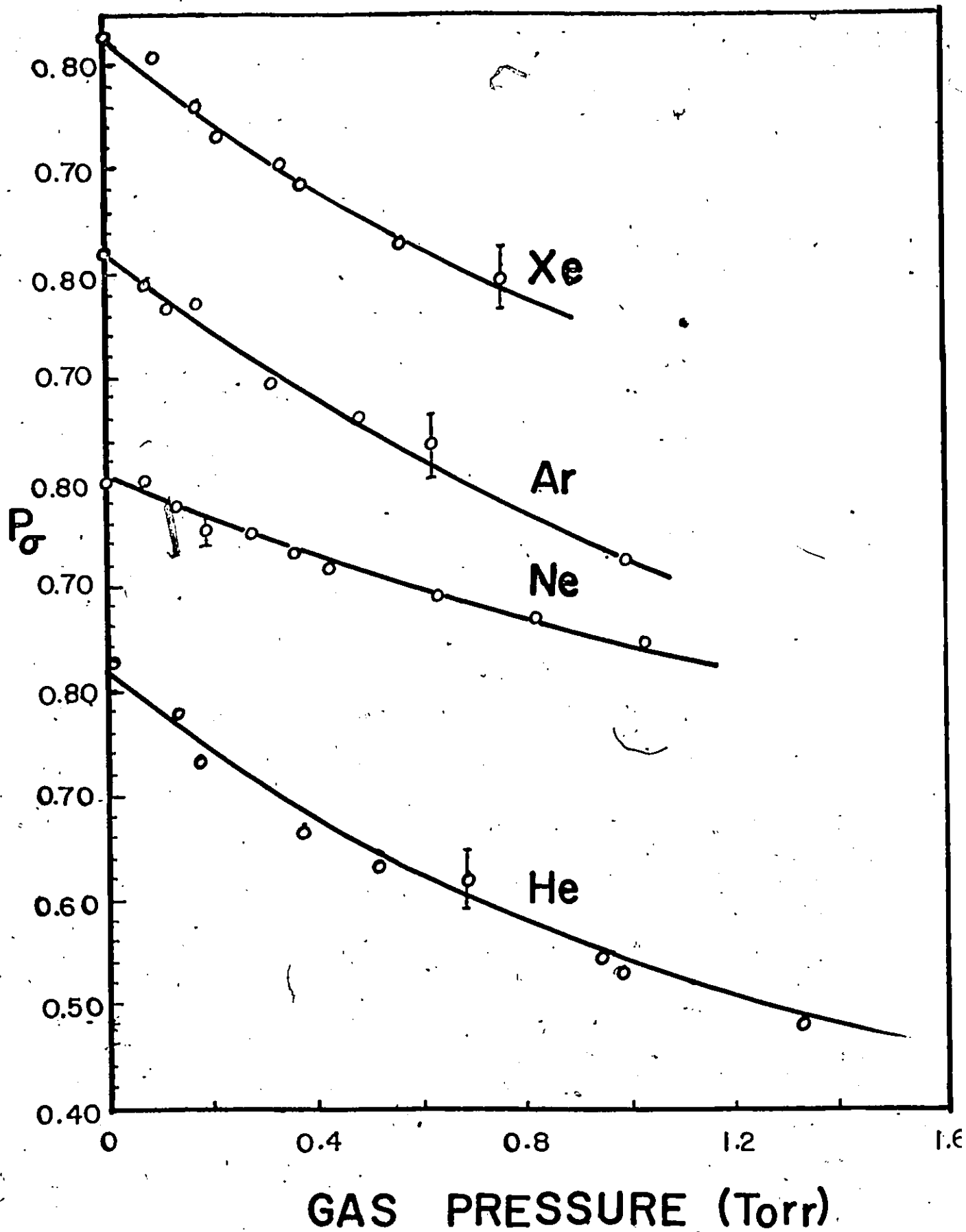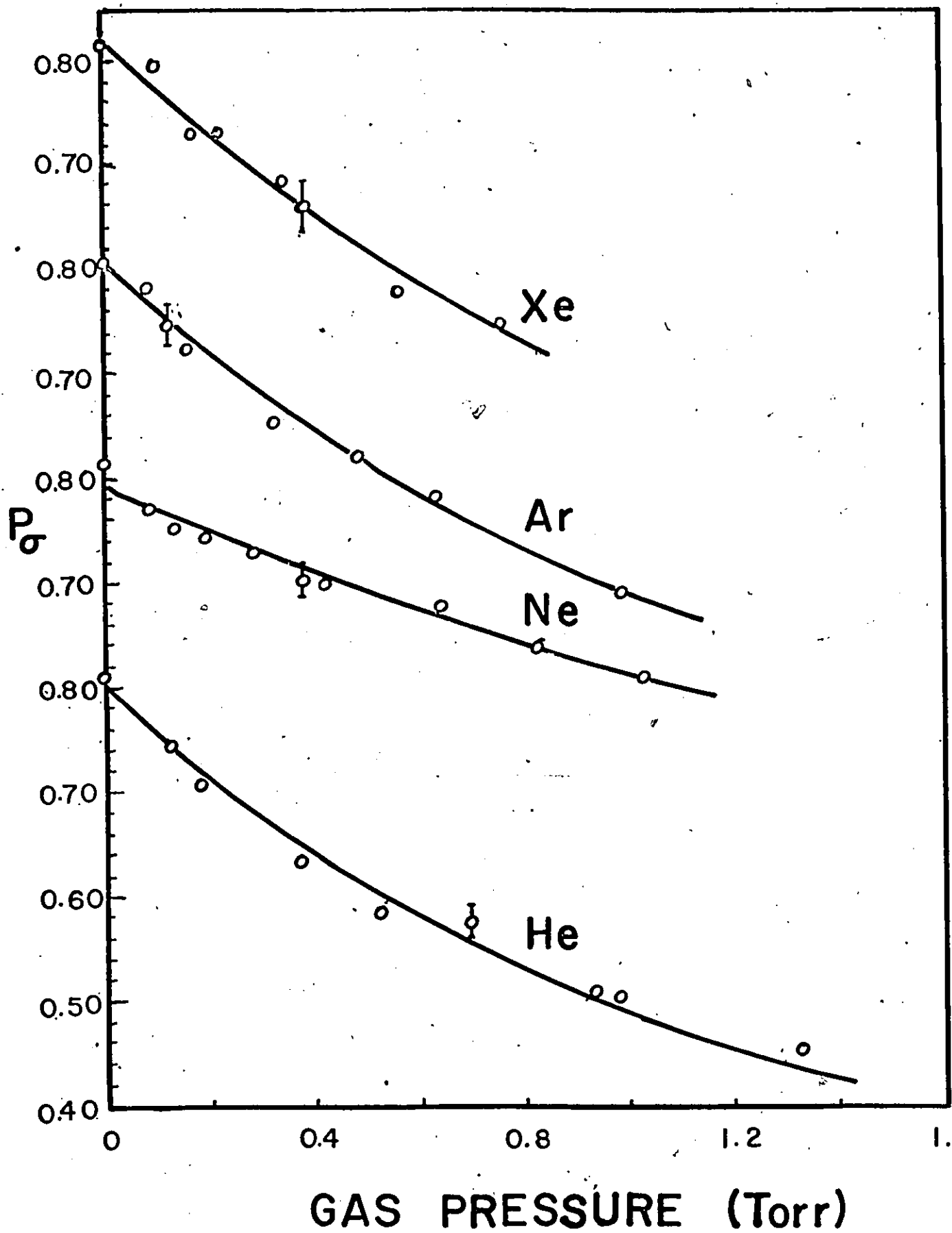
Figure 21.   Variation of the degree of circular

polarization of the 8521-Å resonance fluorescence with

noble gas pressure at 6.7 kG.
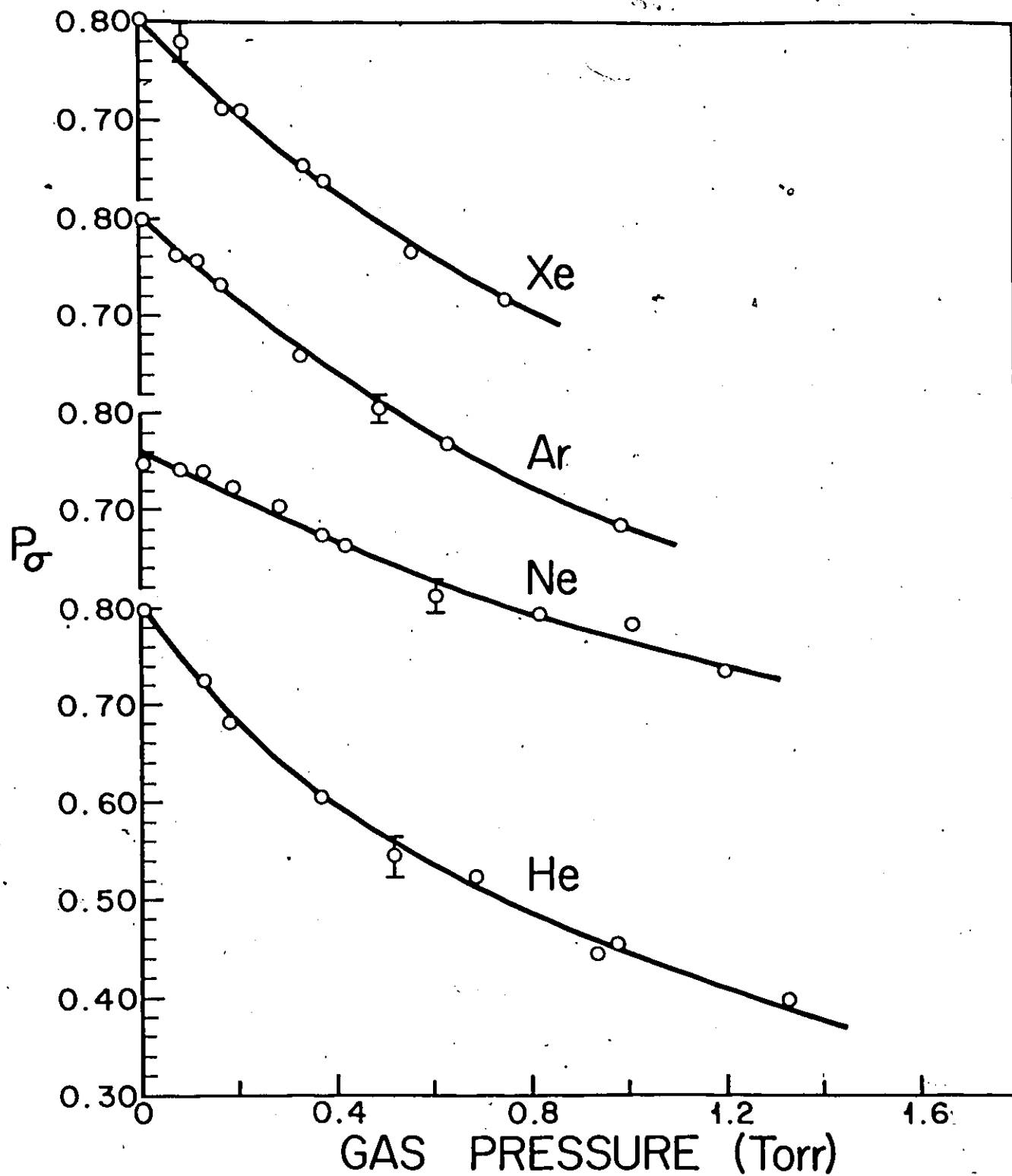
Figure 22.   Variation of the degree of linear

polarization of the 8521-$\overset{o}{A}$ resonance fluorescence with

noble gas pressure at zero field.
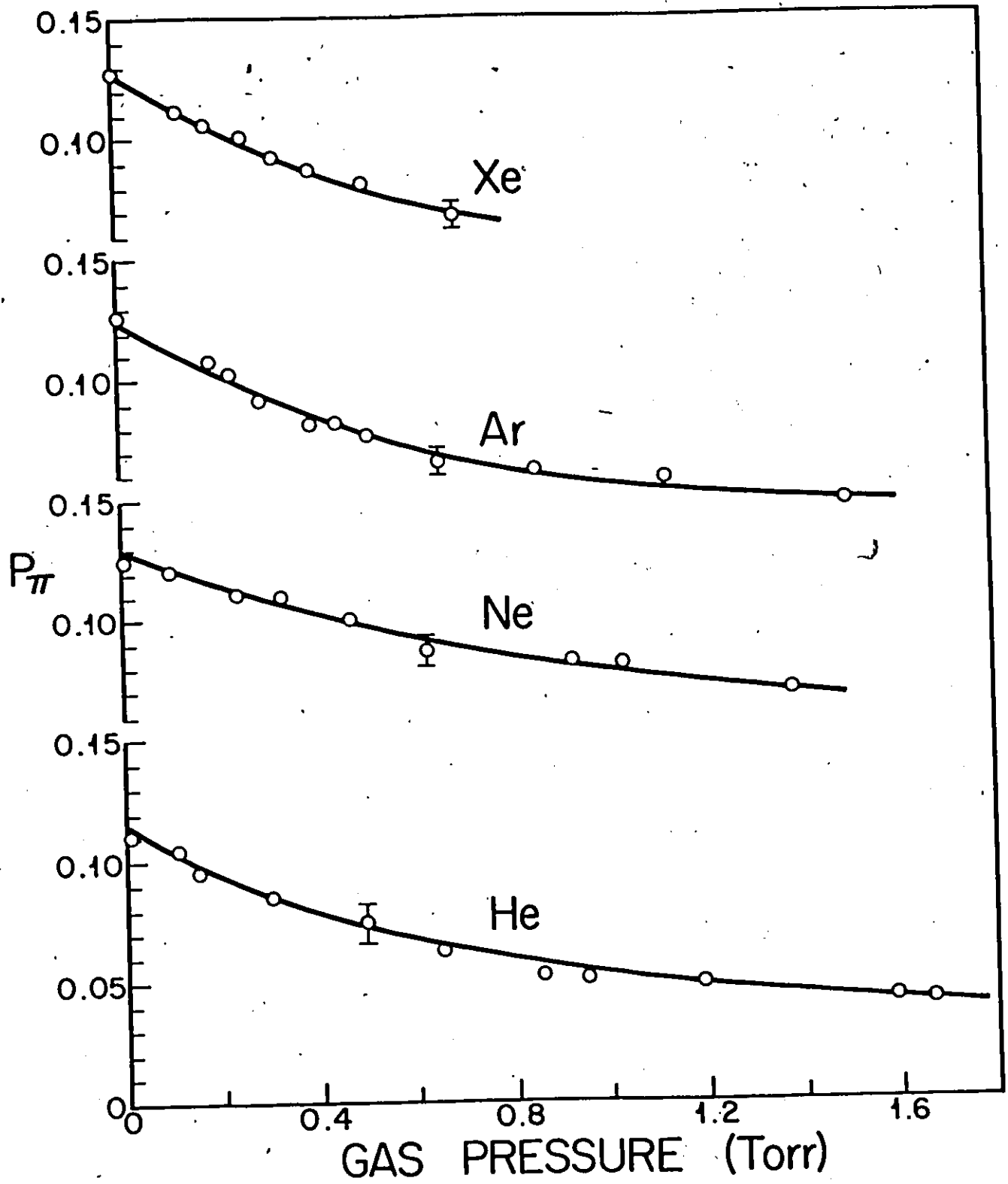
by less than 10%.

The cross sections σ_1 for disorientation and σ_2 for disalignment, derived from least-squares analyses of the experimental results, are listed in Table 5 together with theoretical values calculated by Roueff and Suzor (1974) and by Okunevich and Perel' (1970), and with the disorientation cross sections reported by Fricke et al. (1967) who used the 'J randomization' model to interpret the results of a D_2 optical pumping experiment. Because the latter cross sections are strongly model-dependent, we have also multiplied them by the appropriate factors, corresponding to the two other interaction models, the van der Waals' model and the $m_J \neq -m_J$ selection rule (Papp and Franz 1972; Fricke et al. 1967), and have included the resulting values in Table 5.

The disorientation cross sections measured in high magnetic fields are not significantly different from those yielded by D_2 optical pumping methods which, however, exhibit variations of up to 50%, depending on the model chosen to represent the collisional m_J mixing process. The employment of the 'J randomization' or van der Waals' model in the interpretation of the experimental data produces very similar results which also agree quite well with those obtained in this investigation. On the other hand, the application of the $m_J \neq -m_J$ selection rule leads to much higher cross sections, especially for collisions with He and Ne. When comparing the two sets of experimental results, it should be

TABLE 5.

Cross sections for disorientation (σ_1) and disalignment (σ_2) of $6\,^2P_{3/2}$ Cs atoms, with $\bar{I}$ decoupled

Collision Partners	Magn. Field (kG)	σ_1 (Å²) This investigation	Fricke et al.[10] J rand. v.der Waals		m_J sel. rule	Roueff and Suzor[8]	Okunevich[23]	σ_2/σ_1 This work	σ_2 (Å²) This investigation	Roueff and Suzor[8]	Okunevich[23]
Cs–He	3.8	64 ± 9						1.12±0.15	72 ± 18		
	5.3	80 ± 12	100 ± 19	108 ± 20	150 ± 28	116	55	1.07±0.15	86 ± 21	150	68
	6.7	89 ± 13						0.93±0.14	83 ± 21		
Cs–Ne	3.8	67 ± 10						0.96±0.14	65 ± 16		
	5.3	80 ± 12	91 ± 19	98 ± 20	137 ± 27		99	1.09±0.15	88 ± 22		123
	6.7	98 ± 15						1.29±0.19	126 ± 31		
Cs–Ar	3.8	217 ± 30						1.60±0.24	350 ± 88		
	5.3	234 ± 34	188 ± 40	204 ± 44	282 ± 60		192	1.23±0.18	288 ± 72		238
	6.7	261 ± 39						1.43±0.21	375 ± 94		
Cs–Xe	3.8	317 ± 46						1.62±0.24	514 ± 128		
	5.3	397 ± 60	359 ± 72	389 ± 78	535 ± 108		320	1.68±0.25	668 ± 167		400
	6.7	444 ± 66						1.74±0.26	775 ± 194		

borne in mind that the D_2 optical pumping was carried out in very low magnetic fields, though the authors did take into consideration the presence of nuclear spin. Although the cross sections which I have measured at 5.3 kG and 6.7 kG may be considered equal within experimental error for each buffer gas, the values obtained at 3.8 kG are slightly but significantly lower, possibly because of indeterminate conditions of excitation in this intermediate field. The discrepancy between the theoretical cross sections (for helium) may well be due to different interaction models adopted in the two calculations, but the agreement between the experimental values and those calculated by Okunevich and Perel' (1970) is quite good, though their cross section for helium is rather small in comparison with the other noble gases. The 'J randomization model' predicts $\sigma_2/\sigma_1 = 1$, which is satisfied by our results for He and Ne, but not for Ar and Xe. It is possible that the mechanism of the interaction with the heavier gases is different and involves the m_J selection rule, bearing in mind that its application leads to the prediction $1.5 < \sigma_2/\sigma_1 < 3.$[*]

The disalignment cross sections σ_2 are burdened with a larger error than the σ_1 values, and there are no other experimental data available for comparison, though there is agreement within experimental error, with the calculations of Okunevich and Perel' (1970).

[*] Derived from Equations (28) - (31) in Berdowski et al. 1971.

The cross sections Q(circ.) and Q(lin.) for circular and linear depolarization, obtained at zero field and at 0.6 kG, are presented in Table 6, together with the theoretical spin-coupled values calculated by Rebane and Rebane (1973). At 0.6 kG the nuclear spin should be partly decoupled and the values of Q(circ.) should approach the corresponding σ_1, as is borne out by the results. The agreement between the experimental and theoretical Q(lin.) cross sections is remarkably good except for He; in the case of Q(circ.) at zero field, the situation appears to be just the opposite, with good agreement between the experimental and theoretical values for He, but not for the remaining noble gases.

A scrutiny of all the cross sections listed in Tables 5 and 6, reveals certain trends that may have some general significance. As the magnetic field is increased from zero to kilogauss levels and the nuclear spin becomes decoupled, the depolarization cross sections increase, Q(circ.) and Q(lin.) are representative of σ_1 and σ_2, respectively. That this increase is much more pronounced with Q(circ.) than with Q(lin.), implies a more significant role of the nuclear spin in its effect on the collisional relaxation of the atomic dipole than of the quadrupole. This conclusion has been reached independently by Rebane (1974) in his theoretical analysis of the problem.

It may also be seen that in the cases of virtually all the experimentally determined depolarization cross sections,

TABLE 6

Cross sections for circular and linear depolarization
of $6^2P_{3/2}$ Cs atoms, with $\vec{I}$ coupled

Collision Partner	This Investigation			Rebane & Rebane(1973)	
	$Q(\text{circ.})$ (Å^2)		$Q(\text{lin.})(\text{Å}^2)$	$Q(\text{circ.})$ (Å^2)	$Q(\text{lin.})$ (Å^2)
	zero field	0.6 kG	zero field		
He	38 ± 6	55 ± 9	99 ± 15	42	61
Ne	50 ± 7	77 ± 12	107 ± 16	74	108
Ar	74 ± 12	163 ± 24	260 ± 39	146	212
Xe	125 ± 18	273 ± 40	409 ± 60	240	356

the value for He is quite close to that for Ne, and those
for Ar and Xe are significantly larger and different from
one another. The calculations of Okunevich and Perel' (1970)
and of Rebane and Rebane (1973) do not bear out this par-
ticular feature but, instead, predict Ne cross sections almost
twice as large as the corresponding He values. It is a matter
of conjecture whether this divergence between the experimen-
tal results and theoretical predictions arises from the use
of the van der Waals' model, on which both theoretical treat-
ments were based. This model, when used in the interpretation
of the D_2 optical pumping results (Fricke et al. 1967), still
leads to disorientation cross sections that agree well with
values obtained using the 'J randomization' model, and with
the results of this investigation. It is, perhaps, signifi-
cant that a parallel situation has been reported in the case
of the cross sections for disorientation and disalignment of
$5^2P_{3/2}$ rubidium atoms (Zhitnikov et al. 1970).

3. Sources of Experimental Error

The various cross sections which are collected in
Tables 3, 5 and 6 have been assigned uncertainties ranging
from approximately 15% for the $^2P_{1/2}$ disorientation cross
sections σ_1 measured at 9.8 kG to approximately 25% for the
$^2P_{3/2}$ disalignment cross sections σ_2. The estimates of the
uncertainties ascribed to the particular results were based
on the standard deviations yielded by the lease squares fits
of the raw data taken together with the likely contributions
arising from systematic errors.

Table 7 contains the estimated systematic errors involved in the determination of the degrees of polarization P.

TABLE 7

Systematic errors in the determination
of the degree of polarization P

% Contribution to Systematic Error in P	Source of Error
1	uncertainty in the magnetic field arising from inaccuracy of the gaussmeter and X - Y recorder
1	non-linearity of Y sweep of X - Y recorder and d.c. amplifier or gain of the PAR lock-in
2	determination of the background level
5	uncertainty in the calibration of the McLeod gauge

The magnetic field sweep rate of approximately 20 Gs^{-1}
resulted in negligible distortion of the detected signal
profiles due to time-lag effects.

Statistical errors in the measurement of the photo-
multiplier signals are inferred from the scatter among
individual polarization data determined at specific noble
gas pressures. Such deviations may be as high as 4% and
arise mainly from short term fluctuations in the excitation
intensity.

The uncertainty arising from the data-fitting procedure,
which is reflected in the magnitudes of the standard devi-
ations, is directly correlated with the statistical errors
in the determination of P.

The values of the various cross sections - calculated
on the bases of Equations (III-3), (III-6), (III-21) and
(III-22) - are directly proportional to the slope of Z plotted
against n (see Equation (III-4)). Two systematic errors in
the determination of P - calibration error of the McLeod
gauge and error in the determination of the background level
in the detected photomultiplier signal - directly affect the
determination of the slope. This contribution to the error
in the values for the cross sections is estimated to be 5%
based on the values given in Table 7. Values of the lifetime
τ have uncertainties of approximately 3%. The total error
was obtained by combining the statistical and systematic
errors in quadrature.

VI. SUMMARY AND CONCLUSIONS

Modified Zeeman scanning techniques were used to investigate the depolarization of $6^2P_{1/2}$ and $6^2P_{3/2}$ Cs atoms induced in collisions with ground state noble gas atoms in magnetic fields ranging from zero to 10 kG.

In the case of $6^2P_{1/2}$ atoms, the effect of hfs on the observed dipole relaxation (disorientation) rate was found to be very small, in accord with theoretical predictions appropriate to such depolarization experiments. In contrast, the experimental results yielded by Hanle-effect experiments are strongly affected by nuclear spin-coupling. It thus appears that the significance of the experimentally determined dipole relaxation rates and cross sections may vary depending on the experimental method and on experimental conditions. The cross sections were also found to increase with the strength of the ambient magnetic field, which causes virtual mixing of the $^2P_{1/2}$ and $^2P_{3/2}$ states. It is thus important to bear in mind the two separate effects of the magnetic field on the disorientation cross sections, arising from the decoupling of the nuclear spin and from the virtual fine-structure mixing. For example, in the $5^2P_{1/2}$ Rb atoms the effect of the nuclear spin on the disorientation rate is larger than in the $6^2P_{1/2}$ Cs atoms, and so is the decoupling effect of the magnetic field.

In the case of the $6^2P_{3/2}$ atoms, it was possible to determine separate cross sections for both circular and

linear depolarization which, upon decoupling of the nuclear spin, become representative of the cross sections σ_1 and σ_2. A significant difference was observed in the ratios σ_2/σ_1 between the lighter collision partners (He, Ne) and the heavier ones (Ar, Xe). This difference has not been reported for $^2P_{3/2}$ potassium (Berdowski et al. 1971) or rubidium (Kamke 1975). On the basis of a comparison between various theoretical and experimental cross sections, it seems likely that the depolarization interaction proceeds according to a different mechanism with different noble gas atoms. It is probable that collisions with He and Ne are much 'harder' than for Ar and Xe.

The measured values of Q(lin.) and Q(circ.) for $^2P_{3/2}$ Cs atoms are considerably smaller than their nuclear spin-decoupled counterparts σ_1 and σ_2, indicating that the effect of nuclear spin is more pronounced in the $^2P_{3/2}$ state than in the $^2P_{1/2}$ state, notwithstanding the smaller coupling strength in the $^2P_{3/2}$ state. However, in the $^2P_{3/2}$ state, the increase in the depolarization rate with magnetic field is due almost entirely to the decoupling of the nuclear and electronic spins. This is indicated by the rapid change in the depolarization rate between zero field and 0.6 kG. Above 0.6 kG, the rate of increase is quite small, and the cross sections measured at 0.6 kG and 3.8 kG are of comparable magnitudes; at higher fields, the increase in the cross sections is insignificantly small. Also, the change in the depolarization rate with magnetic field is more pronounced with circular than with

linear polarization, in accord with theoretical predictions
(Rebane 1974).

All the measured cross sections exhibit the charac-
teristic variation with the atomic number of the noble gas
and exhibit a minimum at Ne. It is interesting to note,
however, that this variation is markedly different with the
$^2P_{1/2}$ and $^2P_{3/2}$ states. In the case of the $^2P_{1/2}$ disorientation
cross sections, this variation becomes less pronounced with
increasing atomic number of the alkali atom (Niewitecka and
Krause 1976), whereas in the case of the $^2P_{3/2}$ disorientation
cross sections, the variation becomes more pronounced with
increasing alkali atomic number. The ratios of alkali-noble
gas cross sections $\sigma_1(Xe)/\sigma_1(He)$ are: for Na, 2.2 (Elbel et
al. 1972); for K, 2.9 (Berdowski et al. 1968); for Rb, 3.1
(Kamke 1975) and for Cs, 4.8 (this investigation) or 3.6
(Fricke et al. 1967).

The investigation of depolarization of excited
atoms could be extended by improving the versatility of the
existing apparatus. This could be done by using excitation
sources of different profile widths ranging from "white"
(Franz 1971) to very narrow (laser) together with a magnet,
possibly of the superconducting type, which would be capable
of producing larger fields than those now available. Several
worthwhile depolarization investigations, suggested by the
results of my work, together with that of other authors, could
then be undertaken.

The various multipole decay rates γ_1 could be de-

termined separately and independently. Work is currently underway in this laboratory on selective excitation of a specific m_J sublevel in $4\,^2P_{3/2}$ K atoms, in kilogauss magnetic fields, using narrow-band dye-lasers. A Fabry-Perot interferometer is placed in the fluorescent light beam to detect fluorescent radiation arising from individual Zeeman sublevels, and hence to yield a value for Y_3.

The studies of the magnetic field dependence of the disorientation cross sections for the $^2P_{1/2}$ alkali states could be considerably extended by using the complete range of noble gas collision partners and by extending the region of investigation to much higher magnetic fields. The theory (see Appendix B) predicts a σ_1 'saturation' at a value comparable to that of σ_1 for the $^2P_{3/2}$ atoms. Another promising line of investigation would be to probe the dependence of the $^2P_{3/2}$ depolarization cross sections on buffer gas pressure. Rebane et al. (1971) predict a non-linear dependence on noble gas pressure of Q(lin.) and Q(circ.) for $I \neq 0$, for pressures considerably higher than used in this investigation. They suggest that this effect should arise from the multi-exponential character of the collisionally-induced relaxation.

Continued studies of atomic depolarization should resolve some of the questions raised in the course of this investigation, and provide additional information about the inter-atomic potentials that are involved in the interactions.

APPENDIX A

90

THE LIGHT CHOPPER FOR DETECTION

OF CIRCULAR POLARIZATION

The light chopper was used in conjunction with a lock-in amplifier and, along with a $\lambda/4$ plate, formed part of the circular polarization analyzer in the fluorescent beam at high magnetic fields. The wheel of the chopper had 8 slots, each of which was fitted with a piece of HR polaroid with its transmission axis set perpendicularly to those of its nearest neighbours.

The diagram below represents a plot of signal intensity produced by the analyzer against angle of rotation of the chopper wheel.
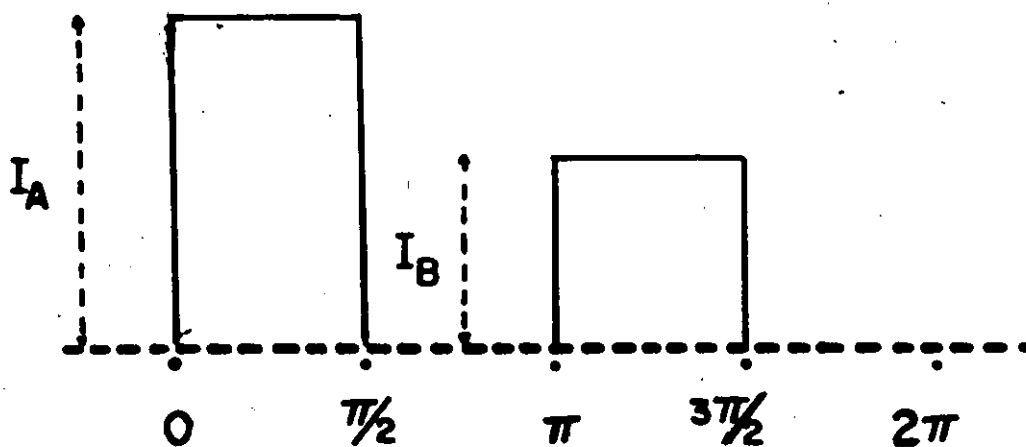
The two maxima I_A and I_B have different peak heights
and represent signals passed by two consecutive slots each
with a different transmission for the polarized light beam.
The two peaks, approximated by square waves for simplicity,
are separated by regions of null intensity at which the light
beam is completely extinguished by the chopping wheel. Since
the pattern repeats itself, the wave form has been represented
with a phase angle ranging from 0 to 2π. The actual chopping
frequency was 333 hz (the chopping frequency refers to the
frequency at which the light beam is extinguished by the chop-
ping wheel) but because alternate slots of the chopping wheel
have different transmissions, the frequency of I_A and/or I_B

is 167 hz.

The output signal of the photomultiplier can be
written as a Fourier function in terms of sine and cosine terms
at integral multiple frequencies of the fundamental 167 hz.

The phase-sensitive detector functions as a Fourier
analyzer in that its output at a particular reference frequency
is proportional to the integrated intensity corresponding to
that frequency. The reference frequency (or its harmonic) is
set equal to either one of the two modulation frequencies in
the detected signal (167 hz or 333 hz).

At the fundamental frequency (167 hz), the output
of the phase-sensitive detector will be proportional to
$(I_A - I_B)$ (the 'difference' signal) and at the second har-

monic frequency (333hz), to $(I_A + I_B)$ (the 'sum' signal).

For the fundamental, we have,

(1) $\quad I_A \int\limits_{0}^{\pi/2} \cos\theta \; d\theta + I_B \int\limits_{\pi}^{3\pi/2} \cos\theta \; d\theta + I_A \int\limits_{0}^{\pi/2} \sin\theta \; d\theta +$

$\quad I_B \int\limits_{\pi}^{3\pi/2} \sin\theta \; d\theta = 2 \; (I_A - I_B).$

For the second harmonic,

(2) $\quad I_A \int\limits_{0}^{\pi} \cos\theta \; d\theta + I_B \int\limits_{2\pi}^{3\pi} \cos\theta \; d\theta + I_A \int\limits_{0}^{\pi} \sin\theta \; d\theta +$

$\quad I_B \int\limits_{2\pi}^{3\pi} \sin\theta \; d\theta = -2 \; (I_A + I_B).$

where the minus sign arises as a phase factor. When a

account coefficien in the

(becomes I_A I_B)

APPENDIX B

THE MAGNETIC FIELD-DEPENDENCE OF THE CROSS SECTIONS σ_1

FOR THE DISORIENTATION OF $^2P_{1/2}$ ALKALI ATOMS

The theoretical treatment of the magnetic field-induced mixing of the $^2P_{1/2}$ and $^2P_{3/2}$ alkali fine structure states is incomplete. The first treatment of this subject (Baylis 1971), using straight line-paths and an R^{-6} repulsive potential, predicted a $B^{0.4}$ variation of σ_1, where B is the magnetic field strength. At magnetic fields of the order of 10 kG, the calculated value of σ_1 for Cs - Ar collisions was approximately $29\overset{\circ}{A}^2$ which is about six times larger than the low field value of $5.1 \overset{\circ}{A}^2$ (Bulos and Happer 1971).

More recently, numerical calculations with improved potentials have been carried out (Baylis 1975) and predict a dependence $\sim B^{1.8}$ of σ_1. Figure 23 shows the variations with magnetic field of the incremental disorientation cross section $\sim kB^{1.8}$ (see Equation (V-1)) plotted against magnetic field for different energies. $\frac{\beta B}{\delta E}$ is the dimensionless field parameter where β is the Bohr magneton, B is the magnetic field strength and δE, the fine structure splitting. This treatment, however, indicates that any change in σ_1 due to the magnetic field should not be observable for values of B less than 10 kG.

The treatment that follows is taken verbatim from the work of W. E. Baylis (1971) and deals with time-reversal

Figure 23.　　Variation with magnetic field of the
Incremental disorientation cross section for the $^2P_{1/2}$
state of Cs, induced in collisions with Ar atoms.
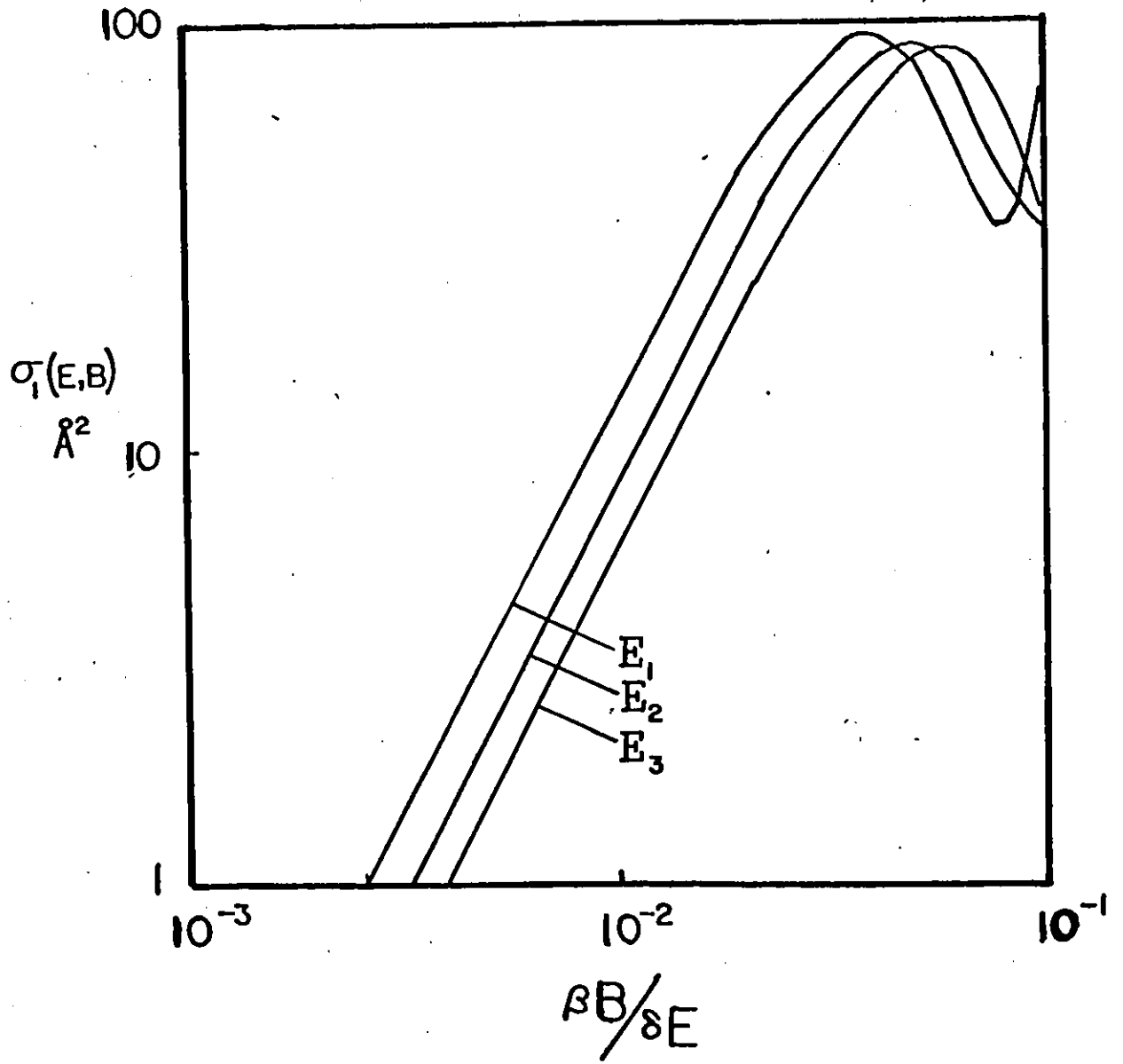
symmetry in classical-path approximations (CPA) and related

selection rules arising in collision-induced transitions.

Special reference is made to depolarization and mixing of

doublet P levels of alkali atoms in thermal collisions with

a noble gas. An external magnetic field is shown to have a

measurable effect on a 'forbidden' transition and to provide

a tool for studying excited-state interatomic potentials.

The usual statement of time-reversal symmetry for

the S matrix is

(1) $\qquad KSK^{+} = S^{+}$

where K is the antilinear time-reversal operator. In time-

independent scattering theory, Equation (1) follows simply from

the time-reversal invariance of the interaction: $KVK^{+} = V$.

In CPA, Equation (1) is true if

(2) $\qquad KV(t)K^{+} = V(-t)$

The condition $KSK^{+} = S^{+}$ is important in collision

theory because of relations which result among matrix elements

of S:

(3) $\qquad \langle jm|S|j'm'\rangle = \langle jm|K^{+}S^{+}K|j'm'\rangle = (-)^{j-m-j'+m'}$
$\langle j'-m'|S|j-m\rangle.$

Thus for example, alkali depolarization in the $P_{1/2}$ state

would be completely forbidden, and more generally, the selec-

tion rule $j,m \neq j,-m$ would hold for systems with an odd number

of electrons (Gallagher 1967 a,b; Franz et al. 1967). Pro-

viding Equation (6) and the CPA are valid, the selection

rule would be rigorous: true to all orders and strengths

of interaction and in any space-fixed reference frame.

Violations of the selection rule are well-known

(Gibbs et al. 1970). The break-down is due to the incor-

rectness of Equation (2). The correct symmetry to expect

in CPA is

$$(4) \qquad KV(t)K^+ = V(t),$$

which does not lead to Equation (3) or to the resulting

selection rule. Nevertheless, matrix elements of $V(t)$ do

obey relations like Equation (3), so that the distinction

between conditions 2 and 4 is not felt until second order

in the S-matrix expansion and there the $V(t) \neq V(-t)$

term is due to coupling with the rotating internuclear axis.

Consequently the selection rule <u>is</u> sometimes weakly obeyed.

In particular, alkali $P_{1/2}$ depolarization must proceed in

second order by mixing with the $P_{3/2}$ state. The δE^{-2} de-

pendence of the $P_{1/2}$ depolarization cross section (Gibbs et

al. 1970) is a consequence.

Some approximations frequently used with CPA

incorrectly preserve the time-reversal symmetry of Equation

(1) and hence lead to erroneous cross sections for inter-

multiplet mixing. Thus any approximation which ignores

rotational coupling is suspect (Nikitin 1969) as is the adia-

batic approximation (Franz et al. 1967). The unitarized

approximation (Callaway and Bauer 1965; Geltman 1969), in which time ordering of interactions is ignored, also gives invalid selection rules if the levels considered are all nearly degenerate.

As an example, one might consider intermultiplet mixing of alkali P states due to collisions with a noble gas.[*] The interaction, dependent on electron position $\underset{\sim}{r}$ and internuclear separation $\underset{\sim}{R}$, is expanded in legendre polynomials:

$$(5) \qquad V(t) = V[\underset{\sim}{r}, \underset{\sim}{R}(t)] = \Sigma(L) \, V^{(L)}[r, R(t)] \, P_L$$
$$[\underset{\sim}{\hat{r}} \cdot \underset{\sim}{\hat{R}}(t)].$$

Only terms with $L = 0,2$ contribute. The cross section $\sigma_L(jj')$ (for relaxation of the Lth multipole of the density matrix in $j \leftrightarrow j$ transitions) is related to the S matrix in an inertial collision frame by[**]

$$(6) \qquad \sigma_L(jj') = 2\pi \int_0^\infty b\,db \, [\delta_{jj'} - \sum_\ell (-)^{L-j-j'+\ell} \begin{Bmatrix} j' & j' & L \\ j & j & \ell \end{Bmatrix} \sum_m$$
$$|S_{\ell m}^{(jj')}|^2]$$

where $S_{\ell m}(jj')$ is the projection of S onto the irreducible tensor $T^{\ell m}(jj')$. In collisions of a heavy alkali with a noble gas, $\sigma_0(1/2 \ 1/2) \ll \sigma_1(1/2 \ 1/2) \ll \sigma_1(3/2 \ 3/2)$.

Application of a magnetic field B of a few thousand gauss further breaks the time-reversal symmetry and slightly

---

[*] Nuclear spin is ignored as it will have no significant effect at fields above 1 kG but may be important at low fields (Happer 1971).

[**] This is an extension of work by A. Omont (1965).

mixes states of different j. The new eigenstates, which
are accurately calculated from perturbation theory, must
be used to find the S matrix for scattering in the field B.
The first order expression for $|\langle 1/2\ 1/2\ |S|1/2\ -\ 1/2\rangle|^2$
averaged over orientations Ω of the collision frame is

$$(7) \qquad \frac{8}{375}\ (\frac{\beta B}{\delta E})^2\ [\ |\int_o^\infty dt \tilde{V}^{(2)}|^2 + 3|\ \int_o^\infty dt\ V^{(2)}\cos 2\varphi|^2]$$

where $\varphi(t)$ is the azimuthal angle of $\underset{\sim}{R}(t)$ in the collision
plane and $\varphi(0)\equiv 0$. To find $1/2\ \sigma_1\ (1/2\ 1/2)$, we integrate
the expression[Equation 7] over impact parameters, replacing
the integrand by the value 2/3 whenever it exceeds unity.

If $V^{(2)}$ varies as R^{-n}, then the depolarization
cross section in the $P_{1/2}$ state is roughly $(\beta B/\delta E)^{2/n-1}$
times those in the $P_{3/2}$ state. Calculations (Baylis 1969)
of CsAr interatomic potentials indicate that for 7 a.u. $\leq R \leq 14$
a.u., $V^{(2)}$ is strongly repulsive whereas the adiabatic $A^2\pi_{1/2}$
potential, which determines the classical path, is relatively
flat. Approximating $V^{(2)}$ by an R^{-6} <u>repulsive</u> potential and
using straight paths, we obtain

$$(8) \qquad \sigma_1\ (\frac{1}{2}\ \frac{1}{2})\ \simeq\ 380\ \overset{o}{A}^2\ (\frac{\beta B}{\delta E}\ \frac{v_o}{v})^{2/5}\ ;$$

where v is the relative velocity, v = 1 km/sec, and δE =
554 kaysers. Thus at 10^4 gauss, where $\beta B/\delta E \simeq 10^{-3}$, $\sigma_1\ (1/2\ 1/2)$
$\simeq 24\overset{o}{A}^2$ which can be compared with the value 5.1 $\overset{o}{A}^2$ measured
at zero gauss (Gallagher 1967[a] a,b).

The dependence of σ_1 (1/2 1/2) on B depends of course on $V^{(2)}$ (R). It may be hoped that further measurements of the field dependence of mixing cross sections will provide additional useful information on on the elusive excited-state interatomic potentials.

BIBLIOGRAPHY

Altman, E.L. and Evdokimov, Yu. V. 1970. Opt. Spectrosc. 29, 431.

Atkinson, R.J., Chapman, G.D. and Krause, L. 1965. J. Opt. Soc. Am., 55, 1269.

Bitter, F., Davis, S. P., Richter, B. and Young, J. E. R. 1954. Phys. Rev. 96, 1531.

Baylis, W. E. 1969. J. Chem. Phys. 51, 2665.

Baylis, W. E. 1971. Abstracts, VII I.C.P.E.A.C. (North-Holland, Amsterdam).

Baylis, W. E. 1975. Private Communication.

Bender, P. L. 1956, Ph.D. Thesis, Princeton University (unpublished).

Berdowski, W., Shiner, T. and Krause, L. 1967. Appl. Opt. 6, 1683.

Berdowski, W. and Krause, L. 1968. Phys Rev. 165, 158.

Berdowski, W., Shiner, T. and Krause, L. 1971. Phys. Rev. A 4, 984.

Breit, G. and Rabi, J. J. 1931. Phys. Rev. 38, 2002.

Buhl, O. 1938. Z. Physik 109, 180, 110, 395.

Bulos, B.R. and Happer, W. 1971. Phys. Rev. A 4, 849.

Chapman, G.D. 1965, Ph.D. Thesis, University of Windsor (unpublished).

Callaway, J. and Bauer, E. 1965. Phys. Rev. A 140, 1072.

Colclough, J. D. 1963, M.Sc. Thesis, University of Windsor, (unpublished).

D'Yakonov, M. I. and Perel', V. I. 1965. Sov. Phys. JETP 20, 997.

D'Yakonov, M. I. and Perel', V. I. 1965. Sov. Phys. JETP 20, 1484.

D'Yakonov, M. I. and Perel', V. I..1965. Sov. Phys. JETP
    21, 227.

Elbel, M. and Naumann, F. 1967. Z. Physik 204, 501, 208,
    104.

Elbel, M., Koch, A. and Schneider, W. 1972. Z. Physik 255,
    14.

Fano, U. 1957. Rev. Mod. Phys. 29, 74.

Franz, F. A. and Franz, J. R. 1966. Phys. Rev. 148, 82.

Franz, F. A., Marshall, T. R. and Munarin, J. A. 1971. Phys.
    Lett. 36A, 31.

Franz, F. A. and Sooriamoorthi, C. E. 1973. Phys. Rev. A 8,
    2390.

Franz, F. A. and Sooriamoorthi, C. E. 1974. Phys. Rev. A 10,
    126.

Fricke, J., Haas, J., Luscher, E. and Franz, F. A. 1967. Phys.
    Rev. 163, 45.

Gallagher, A. 1967. Phys. Rev. 157, 68.

Gallagher, A. 1967. Phys. Rev. 163, 206.

Geltman, S. 1969. Topics in Atomic Collision Theory, p. 199
    (Academic Press, New York).

Gibbs, H. M., Churchill, G. G., Marshall, T. R., Papp, J.F.
    and Franz, F. A. 1970. Phys. Rev. Lett. 25, 263.

Gordeev, E. P., Nikitin, E. E., and Ovchinnikova, M. 1969.
    Can. J. Phys. 47, 1819.

Hanle, W. 1927. Z. Physik 41, 164.

Happer, W. 1971. Private Communication.

Happer, W. 1972. Rev. Mod. Phys. 144, 169.

Kastler, A. 1950. J. Phys. Rad. 11, 255.

Kamke, B. 1975. Z. Physik A273, 23.

Krause, L. 1966. Appl. Opt. 5, 1375.

Link, J. 1966. J. Opt. Soc. Am. 56, 1195.

Mandelberg, H. I. 1968. Proceedings of the Conference on Heavy Particle Collisions, Belfast, p. 177 (unpublished).

Markova, G. V. and Chaika, M. P. 1967. Opt. Spectrosc. 23, 456.

Marrus, R. and Yellin, J. 1966. Phys. Rev. 141, 130.

Niewitecka, B., Skalinski, T. and Krause, L. 1974. Can. J. Phys. 52, 1956.

Niewitecka, B. and Krause, L. 1975. Can. J. Phys. 53, 1499.

Niewitecka, B. and Krause, L. 1976. Can. J. Phys. (to be published).

Nikitin, E. E. 1969. Comments At. Mol. Phys. 1, 122.

Okunevich, A. I. and Perel' V. I. 1970. Sov. Phys. JETP 31, 356.

Omont, A. 1965. J. Physique 26, 26.

Papp, J. F. and Franz, F. A. 1972. Phys. Rev. A 5, 1973.

Rebane, V. N., Rebane, T. K. and Cherenkovskii, V. A. 1972. Opt. Spectrosc. 33, 337.

Rebane, V. N. and Rebane, T. K. 1972. Opt. Spectrosc. 34, 378.

Rebane, V. N. 1974. Opt. Spectrosc. 36, 598.

Roueff, E. and Suzor, A. 1974. J. Physique 35, 727.

Stern, D. and Volmer, M. 1919. Z. Physik 20, 183.

Sooriamoorthi, C. E. 1974, Ph.D. Thesis, Indiana University.

Wang, C. H. and Tomlinson, W. J. 1969. Phys. Rev. 181, 115.

Wood, R. W. 1922. Phil. Mag. 44, 1109.

Wood, R.W. 1923. Proc. Roy. Soc. 103, 396.

Zhitnikov, R. A., Kuleshov, P. P., Okunevich, A. I. and Sevast'yanov, B. N. 1970. Sov. Phys. JETP 31, 445.

VITA AUCTORIS

I was born on February 18, 1944 in Chatham, Ontario. I attended primary and secondary schools in Windsor, Ontario and after graduation in 1962, I attended the University of Windsor. In 1966, I graduated from an Honours Physics course and enrolled in the Faculty of Graduate Studies to work toward a Master of Science degree which I obtained in 1968.